

# $B_{s,d} \rightarrow \pi\pi, \pi K, KK$ : Status and Prospects

Robert Fleischer

Theory Division, Department of Physics, CERN, CH-1211 Geneva 23, Switzerland

## Abstract

Several years ago, it was pointed out that the  $U$ -spin-related decays  $B_d \rightarrow \pi^+\pi^-$ ,  $B_s \rightarrow K^+K^-$  and  $B_d \rightarrow \pi^\mp K^\pm$ ,  $B_s \rightarrow \pi^\pm K^\mp$  offer interesting strategies for the extraction of the angle  $\gamma$  of the unitarity triangle. Using the first results from the Tevatron on the  $B_s$  decays and the  $B$ -factory data on  $B_{u,d}$  modes, we compare the determinations of  $\gamma$  from both strategies, study the sensitivity on  $U$ -spin-breaking effects, discuss the resolution of discrete ambiguities, predict observables that were not yet measured but will be accessible at LHCb, explore the extraction of the width difference  $\Delta\Gamma_s$  from untagged  $B_s \rightarrow K^+K^-$  rates, and address the impact of new physics. The data for the  $B_d \rightarrow \pi^+\pi^-$ ,  $B_s \rightarrow K^+K^-$  system favour the BaBar measurement of direct CP violation in  $B_d \rightarrow \pi^+\pi^-$ , which will be used in the numerical analysis, and result in a fortunate situation, yielding  $\gamma = (66.6_{-5.0-3.0}^{+4.3+4.0})^\circ$ , where the latter errors correspond to a generous estimate of  $U$ -spin-breaking effects. On the other hand, the  $B_d \rightarrow \pi^\mp K^\pm$ ,  $B_s \rightarrow \pi^\pm K^\mp$  analysis leaves us with  $26^\circ \leq \gamma \leq 70^\circ$ , and points to a value of the  $B_s \rightarrow \pi^\pm K^\mp$  branching ratio that is larger than the current Tevatron result. An important further step will be the measurement of mixing-induced CP violation in  $B_s \rightarrow K^+K^-$ , which will also allow us to extract the  $B_s^0$ - $\bar{B}_s^0$  mixing phase unambiguously with the help of  $B_s \rightarrow J/\psi\phi$  at the LHC. Finally, the measurement of direct CP violation in  $B_s \rightarrow K^+K^-$  will make the full exploitation of the physics potential of the  $B_{s,d} \rightarrow \pi\pi, \pi K, KK$  modes possible.



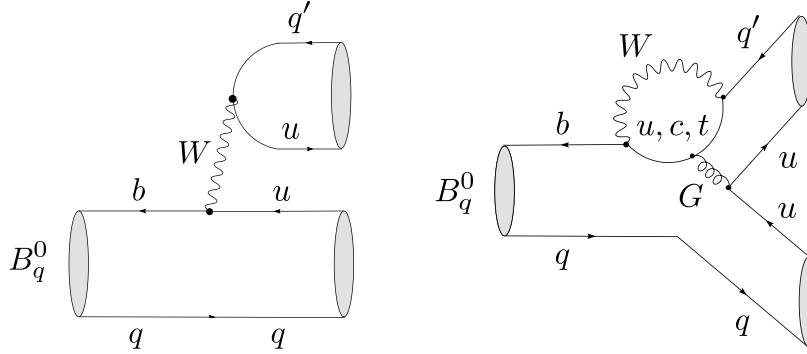


Figure 1: Tree and penguin topologies contributing to the  $U$ -spin-related  $B_d^0 \rightarrow \pi^+\pi^-$ ,  $B_s^0 \rightarrow K^+K^-$  and  $B_d^0 \rightarrow \pi^-K^+$ ,  $B_s^0 \rightarrow \pi^+K^-$  decays ( $q, q' \in \{d, s\}$ ).

## 1 Introduction

Decays of  $B$  mesons into two light pseudoscalar mesons offer interesting probes for the exploration of CP violation. The key problem in these studies is usually given by the hadronic matrix elements of local four-quark operators, which suffer from large theoretical uncertainties. In 1999 [1], it was pointed that the system of the  $B_d^0 \rightarrow \pi^+\pi^-$  and  $B_s^0 \rightarrow K^+K^-$  decays is particularly interesting in this respect. These transitions, which receive contributions from tree and penguin topologies, allow us to determine the angle  $\gamma$  of the unitarity triangle (UT) of the Cabibbo–Kobayashi–Maskawa (CKM) matrix [2] with the help of the  $U$ -spin symmetry, which is a subgroup of the  $SU(3)_F$  flavour symmetry of strong interactions, connecting the strange and down quarks in the same way through  $SU(2)$  transformations as the isospin symmetry connects the up and down quarks. As can be seen in Fig. 1, the  $B_d^0 \rightarrow \pi^+\pi^-$  and  $B_s^0 \rightarrow K^+K^-$  modes are related to each other through an interchange of all down and strange quarks. Consequently, the  $U$ -spin flavour symmetry allows us to derive relations between their hadronic parameters so that the experimental observables offer sufficient information to extract them and the UT angle  $\gamma$  from the data. The advantage of this  $U$ -spin strategy with respect to the conventional  $SU(3)$  flavour-symmetry strategies [3] is twofold:

- no additional dynamical assumptions such as the neglect of annihilation topologies have to be made, which could be spoiled by large rescattering effects;
- electroweak (EW) penguin contributions, which are not invariant under the isospin symmetry because of the different up- and down-quark charges, can be included.

The theoretical accuracy is therefore only limited by non-factorizable  $U$ -spin-breaking effects, as the factorizable corrections can be taken into account through appropriate ratios of form factors and decay constants. Moreover, we have key relations between certain hadronic parameters, where these quantities cancel. Interestingly, also experimental insights into  $U$ -spin-breaking effects can be obtained, which do not indicate any anomalous enhancement.

The relevant observables are the CP-averaged branching ratios as well as the direct and mixing-induced CP asymmetries  $\mathcal{A}_{\text{CP}}^{\text{dir}}(B_q \rightarrow f)$  and  $\mathcal{A}_{\text{CP}}^{\text{mix}}(B_q \rightarrow f)$ , respectively, en-

tering the following time-dependent rate asymmetries for decays into CP eigenstates [4]:

$$\begin{aligned}\mathcal{A}_{\text{CP}}(t) &\equiv \frac{\Gamma(B_q^0(t) \rightarrow f) - \Gamma(\bar{B}_q^0(t) \rightarrow f)}{\Gamma(B_q^0(t) \rightarrow f) + \Gamma(\bar{B}_q^0(t) \rightarrow f)} \\ &= \left[ \frac{\mathcal{A}_{\text{CP}}^{\text{dir}}(B_q \rightarrow f) \cos(\Delta M_q t) + \mathcal{A}_{\text{CP}}^{\text{mix}}(B_q \rightarrow f) \sin(\Delta M_q t)}{\cosh(\Delta \Gamma_q t/2) - \mathcal{A}_{\Delta \Gamma}(B_q \rightarrow f) \sinh(\Delta \Gamma_q t/2)} \right],\end{aligned}\quad (1.1)$$

where  $\Delta M_q$  and  $\Delta \Gamma_q$  are the mass and width differences of the  $B_q$  mass eigenstates, respectively. Throughout this paper, we shall apply a sign convention for CP asymmetries that is similar to (1.1), also for the direct CP asymmetries of  $B$  decays into flavour-specific final states.

As can be seen in Fig. 1, there is yet another pair of  $U$ -spin-related  $B_{d,s}$  decays that is mediated by the same quark transitions:  $B_d^0 \rightarrow \pi^- K^+$  and  $B_s^0 \rightarrow \pi^+ K^-$ . In contrast to the  $B_d^0 \rightarrow \pi^+ \pi^-$ ,  $B_s^0 \rightarrow K^+ K^-$  system, the final states are flavour-specific. Consequently, we have to rely on the direct CP-violating rate asymmetry as no mixing-induced CP violation arises. If additional information provided by the  $B^+ \rightarrow \pi^+ K^0$  channel is used, together with plausible dynamical assumptions about final-state interaction effects and colour-suppressed EW penguin topologies, the  $U$ -spin-related  $B_d^0 \rightarrow \pi^- K^+$ ,  $B_s^0 \rightarrow \pi^+ K^-$  decays also allow the extraction of the CKM angle  $\gamma$  [5].

Thanks to the  $e^+e^-$   $B$  factories with the BaBar (SLAC) and Belle (KEK) experiments, the  $B^\pm$  and  $B_d$  decays are now experimentally well established, with the following CP-averaged branching ratios, as compiled by the Heavy Flavour Averaging Group (HFAG) [6]:

$$\text{BR}(B_d \rightarrow \pi^+ \pi^-) = (5.16 \pm 0.22) \times 10^{-6}, \quad (1.2)$$

$$\text{BR}(B_d \rightarrow \pi^\mp K^\pm) = (19.4 \pm 0.6) \times 10^{-6}, \quad (1.3)$$

$$\text{BR}(B^\pm \rightarrow \pi^\pm K) = (23.1 \pm 1.0) \times 10^{-6}. \quad (1.4)$$

The  $B_d \rightarrow \pi^\mp K^\pm$  channel led to the observation of direct CP violation in the  $B$ -meson system [7], where the current HFAG average reads as

$$\mathcal{A}_{\text{CP}}^{\text{dir}}(B_d \rightarrow \pi^\mp K^\pm) = 0.095 \pm 0.013. \quad (1.5)$$

Concerning the measurements of CP violation in  $B_d^0 \rightarrow \pi^+ \pi^-$ , the BaBar and Belle collaborations agree now perfectly on the mixing-induced CP asymmetry:

$$\mathcal{A}_{\text{CP}}^{\text{mix}}(B_d \rightarrow \pi^+ \pi^-) = \begin{cases} 0.60 \pm 0.11 \pm 0.03 \text{ (BaBar [8])} \\ 0.61 \pm 0.10 \pm 0.04 \text{ (Belle [9])}, \end{cases} \quad (1.6)$$

yielding the average of  $\mathcal{A}_{\text{CP}}^{\text{mix}}(B_d \rightarrow \pi^+ \pi^-) = 0.61 \pm 0.08$  [6]. On the other hand, the picture of direct CP violation is still not experimentally settled, and the corresponding  $B$ -factory measurements differ at the  $2.6\sigma$  level:

$$\mathcal{A}_{\text{CP}}^{\text{dir}}(B_d \rightarrow \pi^+ \pi^-) = \begin{cases} -0.21 \pm 0.09 \pm 0.02 \text{ (BaBar [8])} \\ -0.55 \pm 0.08 \pm 0.05 \text{ (Belle [9])}. \end{cases} \quad (1.7)$$

In a recent paper [10], it was pointed out that the branching ratio and direct CP asymmetry of the  $B_d^0 \rightarrow \pi^- K^+$  mode favour actually the BaBar result. Following a different avenue, we will arrive at the same conclusion.

Since the  $e^+e^-$   $B$  factories are operated at the  $\Upsilon(4S)$  resonance,  $B_s$  decays could not be studied at these colliders.<sup>1</sup> The exploration of the  $B_s$  system is the territory of hadron colliders, i.e. of the Tevatron (FNAL), which is currently taking data, and of the LHC (CERN), which will start operation soon. In fact, signals for the  $B_s^0 \rightarrow K^+ K^-$  and  $B_s^0 \rightarrow \pi^+ K^-$  decays were recently observed at the Tevatron by the CDF collaboration at the  $4\sigma$  and  $5\sigma$  levels, respectively, which correspond to the following CP-averaged branching ratios: [12, 13]:

$$\text{BR}(B_s \rightarrow \pi^\pm K^\mp) = (5.00 \pm 0.75 \pm 1.0) \times 10^{-6}, \quad (1.8)$$

$$\text{BR}(B_s \rightarrow K^+ K^-) = (24.4 \pm 1.4 \pm 4.6) \times 10^{-6}. \quad (1.9)$$

Moreover, also a CP violation measurement is available:

$$\mathcal{A}_{\text{CP}}^{\text{dir}}(B_s \rightarrow \pi^\pm K^\mp) = -0.39 \pm 0.15 \pm 0.08, \quad (1.10)$$

whereas results for the CP-violating observables of  $B_s \rightarrow K^+ K^-$  were not yet reported.

In view of this progress, it is interesting to confront the  $B_d \rightarrow \pi^+ \pi^-$ ,  $B_s \rightarrow K^+ K^-$  and  $B_d \rightarrow \pi^\mp K^\pm$ ,  $B_s \rightarrow \pi^\pm K^\mp$  strategies with the measurements performed at the  $B$  factories and the Tevatron. This is also an important analysis in view of the quickly approaching start of the LHC with its dedicated  $B$ -decay experiment LHCb, where the physics potential of the  $B_s$ -meson system can be fully exploited [14]. We will therefore give a detailed presentation, collecting also the relevant formulae, which should be helpful for the analysis of the future improved experimental data. The outline of this paper is as follows: in Section 2, we have a closer look at the  $B_d \rightarrow \pi^+ \pi^-$ ,  $B_s \rightarrow K^+ K^-$  strategy, and move on to the  $B_d \rightarrow \pi^\mp K^\pm$ ,  $B_s \rightarrow \pi^\pm K^\mp$  system in Section 3. Finally, we summarize our conclusions in Section 4. For analyses using QCD factorization, soft collinear effective theory or perturbative QCD, the reader is referred to Refs. [15–17].

## 2 The $B_d \rightarrow \pi^+ \pi^-$ , $B_s \rightarrow K^+ K^-$ Strategy

### 2.1 CP Violation in $B_d \rightarrow \pi^+ \pi^-$

In the Standard Model (SM), using the unitarity of the CKM matrix, the transition amplitude of the  $B_d^0 \rightarrow \pi^+ \pi^-$  decay can be written as follows [1]:

$$A(B_d^0 \rightarrow \pi^+ \pi^-) = e^{i\gamma} \left(1 - \frac{\lambda^2}{2}\right) \mathcal{C} [1 - d e^{i\theta} e^{-i\gamma}], \quad (2.1)$$

where  $\gamma$  is the corresponding angle of the UT,  $\lambda$  the parameter of the Wolfenstein expansion of the CKM matrix [18],  $\mathcal{C}$  denotes a CP-conserving strong amplitude that is

---

<sup>1</sup>Recently, data were taken by Belle at  $\Upsilon(5S)$ , allowing also access to  $B_s$  decays [11].

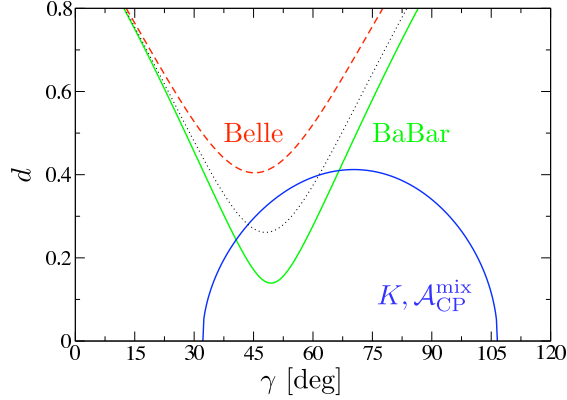


Figure 2: The contours in the  $\gamma$ - $d$  plane that follow from the central values of the BaBar and Belle measurements of the CP asymmetries of the  $B_d \rightarrow \pi^+\pi^-$  channel and the ratio of the CP-averaged  $B_d \rightarrow \pi^+\pi^-$ ,  $B_s \rightarrow K^+K^-$  branching ratios. The dotted line corresponds to the HFAG average for the direct CP violation in  $B_d \rightarrow \pi^+\pi^-$ .

governed by the tree contributions, while the CP-conserving hadronic parameter  $d e^{i\theta}$  measures – sloppily speaking – the ratio of penguin to tree amplitudes. The CP asymmetries introduced in (1.1) take then the following form:

$$\mathcal{A}_{\text{CP}}^{\text{dir}}(B_d \rightarrow \pi^+\pi^-) = - \left[ \frac{2 d \sin \theta \sin \gamma}{1 - 2 d \cos \theta \cos \gamma + d^2} \right] \quad (2.2)$$

$$\mathcal{A}_{\text{CP}}^{\text{mix}}(B_d \rightarrow \pi^+\pi^-) = + \left[ \frac{\sin(\phi_d + 2\gamma) - 2 d \cos \theta \sin(\phi_d + \gamma) + d^2 \sin \phi_d}{1 - 2 d \cos \theta \cos \gamma + d^2} \right], \quad (2.3)$$

where  $\phi_d$  is the CP-violating  $B_d^0$ - $\bar{B}_d^0$  mixing phase, which is given by  $2\beta$  in the SM, with  $\beta$  denoting another UT angle. This phase has been measured at the  $B$  factories with the help of the “golden” decay  $B_d^0 \rightarrow J/\psi K_S$  and similar modes, including  $B_d \rightarrow J/\psi K^*$  and  $B_d \rightarrow D^* D^* K_S$  channels to resolve a twofold ambiguity, as follows [6]:

$$\phi_d = (42.6 \pm 2)^\circ. \quad (2.4)$$

The general expressions in (2.2) and (2.3) allow us to eliminate the strong phase  $\theta$ , and to calculate  $d$  as a function of  $\gamma$  by using the formulae given in Ref. [1]. In Fig. 2, we show the corresponding contours for the central values of the BaBar and Belle results in (1.6) and (1.7). In order to guide the eye, we have also included the contour (dotted line) representing the central value of the HFAG average  $\mathcal{A}_{\text{CP}}^{\text{dir}}(B_d \rightarrow \pi^+\pi^-) = -0.38 \pm 0.07$  of the BaBar and Belle results for the direct CP violation in  $B_d \rightarrow \pi^+\pi^-$  [6]. It should be emphasized that these contours are valid *exactly* in the SM.

## 2.2 CP-Averaged $B_s \rightarrow K^+K^-$ , $B_d \rightarrow \pi^+\pi^-$ Branching Ratios

Let now  $B_s^0 \rightarrow K^+K^-$  enter the stage. In analogy to (2.1), the corresponding decay amplitude can be written as

$$A(B_s^0 \rightarrow K^+K^-) = e^{i\gamma} \lambda \mathcal{C}' \left[ 1 + \frac{1}{\epsilon} d' e^{i\theta'} e^{-i\gamma} \right], \quad (2.5)$$

where

$$\epsilon \equiv \frac{\lambda^2}{1 - \lambda^2} = 0.05, \quad (2.6)$$

and  $\mathcal{C}'$  and  $d'e^{i\theta'}$  are the  $B_s^0 \rightarrow K^+K^-$  counterparts of the  $B_d^0 \rightarrow \pi^+\pi^-$  parameters  $\mathcal{C}$  and  $de^{i\theta}$ , respectively. If we apply the  $U$ -spin symmetry, we obtain the following relations [1]:

$$d' = d, \quad \theta' = \theta. \quad (2.7)$$

As was also pointed out in Ref. [1], these relations are not affected by factorizable  $U$ -spin-breaking corrections, i.e. the relevant form factors and decay constants cancel. This feature holds also for chirally enhanced contributions to the transition amplitudes.

Since the CP asymmetries of the  $B_s^0 \rightarrow K^+K^-$  decay have not yet been measured, we have to use the CP-averaged branching ratio of this mode, which also provides valuable information. For the determination of  $\gamma$ , it is useful to introduce the quantity

$$K = \frac{1}{\epsilon} \left| \frac{\mathcal{C}}{\mathcal{C}'} \right|^2 \left[ \frac{M_{B_s}}{M_{B_d}} \frac{\Phi(M_\pi/M_{B_d}, M_\pi/M_{B_d})}{\Phi(M_K/M_{B_s}, M_K/M_{B_s})} \frac{\tau_{B_d}}{\tau_{B_s}} \right] \left[ \frac{\text{BR}(B_s \rightarrow K^+K^-)}{\text{BR}(B_d \rightarrow \pi^+\pi^-)} \right], \quad (2.8)$$

where

$$\Phi(x, y) \equiv \sqrt{[1 - (x + y)^2][1 - (x - y)^2]} \quad (2.9)$$

is the well-known  $B \rightarrow PP$  phase-space function, and the  $\tau_{B_{d,s}}$  are the  $B_{d,s}$  lifetimes. Applying the relations in (2.7), we arrive at

$$K = \frac{1}{\epsilon^2} \left[ \frac{\epsilon^2 + 2\epsilon d \cos \theta \cos \gamma + d^2}{1 - 2d \cos \theta \cos \gamma + d^2} \right]. \quad (2.10)$$

If we combine  $K$  with  $\mathcal{A}_{\text{CP}}^{\text{mix}}(B_d \rightarrow \pi^+\pi^-)$ , which depend both on  $d \cos \theta$ , we can fix another contour in the  $\gamma$ - $d$  plane with the help of the formulae given in Ref. [1].

In order to determine  $K$  from the CP-averaged branching ratios, the  $U$ -spin-breaking corrections to the ratio  $|\mathcal{C}'/\mathcal{C}|$ , which equals 1 in the strict  $U$ -spin limit, have to be determined. In contrast to the  $U$ -spin relations in (2.7),  $|\mathcal{C}'/\mathcal{C}|$  involves hadronic form factors in the factorization approximation:

$$\left| \frac{\mathcal{C}'}{\mathcal{C}} \right|_{\text{fact}} = \frac{f_K}{f_\pi} \frac{F_{B_s K}(M_K^2; 0^+)}{F_{B_d \pi}(M_\pi^2; 0^+)} \left( \frac{M_{B_s}^2 - M_K^2}{M_{B_d}^2 - M_\pi^2} \right), \quad (2.11)$$

where  $f_K$  and  $f_\pi$  denote the kaon and pion decay constants, and  $F_{B_s K}(M_K^2; 0^+)$  and  $F_{B_d \pi}(M_\pi^2; 0^+)$  parametrize the hadronic quark-current matrix elements  $\langle K^- | (\bar{b}u)_{V-A} | B_s^0 \rangle$  and  $\langle \pi^- | (\bar{b}u)_{V-A} | B_d^0 \rangle$ , respectively [19]. These quantities were analyzed using QCD sum-rule techniques in detail in Ref. [20], yielding

$$\left| \frac{\mathcal{C}'}{\mathcal{C}} \right|_{\text{fact}}^{\text{QCDSR}} = 1.52_{-0.14}^{+0.18}. \quad (2.12)$$

As we will see in Section 3, we can actually determine this quantity with the help of the data for the  $B_d \rightarrow \pi^\mp K^\pm$ ,  $B_s \rightarrow \pi^\pm K^\mp$  system. Since the corresponding value agrees remarkably well with (2.12), large non-factorizable  $U$ -spin-breaking effects are disfavoured, which gives us further confidence in applying (2.7).

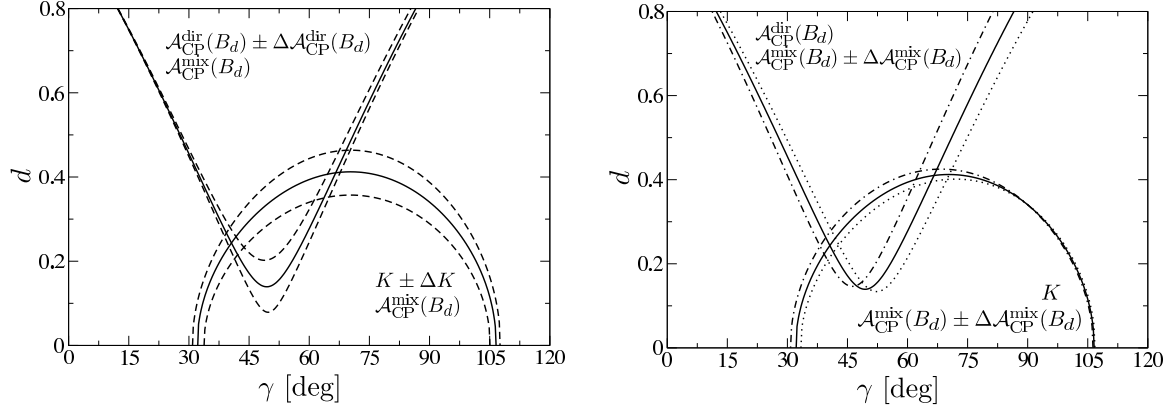


Figure 3: Contours in the  $\gamma$ - $d$  plane fixed through the CP asymmetries of  $B_d^0 \rightarrow \pi^+\pi^-$  for the BaBar result of direct CP violation and the quantity  $K$ : the left panel shows the  $1\sigma$  ranges of  $K$  (upper and lower curves correspond to  $K = 51.30$  and  $30.76$ , respectively) and  $\mathcal{A}_{\text{CP}}^{\text{dir}}(B_d \rightarrow \pi^+\pi^-)$  (upper and lower curves correspond to  $\mathcal{A}_{\text{CP}}^{\text{dir}} = -0.30$  and  $-0.12$ , respectively), whereas the right panel shows the  $1\sigma$  range of  $\mathcal{A}_{\text{CP}}^{\text{mix}}(B_d \rightarrow \pi^+\pi^-)$  (dot-dashed and dotted curves correspond to  $\mathcal{A}_{\text{CP}}^{\text{mix}} = 0.69$  and  $0.53$ , respectively).

## 2.3 Extraction of $\gamma$ and Hadronic Parameters

If we use (1.2) and (1.9) with (2.12) and add the errors in quadrature, we obtain

$$K = 41.03 \pm 10.27. \quad (2.13)$$

In Fig. 2, we have also included the contour following from the central values of  $K$  and  $\mathcal{A}_{\text{CP}}^{\text{mix}}(B_d \rightarrow \pi^+\pi^-)$ . We see that the intersections with the  $\mathcal{A}_{\text{CP}}^{\text{dir}}(B_d \rightarrow \pi^+\pi^-)$ - $\mathcal{A}_{\text{CP}}^{\text{mix}}(B_d \rightarrow \pi^+\pi^-)$  contour following from the BaBar data give a twofold solution for  $\gamma$  around  $41^\circ$  and  $67^\circ$ , whereas we obtain no intersection with the corresponding Belle curve. Consequently, the measured  $B_s \rightarrow K^+K^-$  branching ratio disfavors the Belle result for the direct CP violation in  $B_d^0 \rightarrow \pi^+\pi^-$ . A similar observation was also made in Ref. [10], using, however, a different avenue. For the following analysis, we will therefore only use the BaBar measurement of  $\mathcal{A}_{\text{CP}}^{\text{dir}}(B_d \rightarrow \pi^+\pi^-)$ , which covers also the prediction for this asymmetry made in Ref. [10] within the uncertainties.

In Fig. 3, we show impact of the uncertainties of  $K$  and the CP asymmetries of  $B_d^0 \rightarrow \pi^+\pi^-$ . We obtain the following numerical results:

$$\begin{aligned} \gamma &= (40.6^{+1.6+1.1+2.3}_{-1.3-0.6-2.4})^\circ = (40.6^{+3.0}_{-2.8})^\circ, \\ d &= 0.243^{+0.024+0.015+0.002}_{-0.028-0.008-0.001} = 0.243^{+0.028}_{-0.029}, \\ \theta &= (29.2^{+5.5+14.2+1.7}_{-3.5-12.8-1.3})^\circ = (29.2^{+15.3}_{-13.3})^\circ, \end{aligned} \quad (2.14)$$

$$\begin{aligned} \gamma &= (66.6^{+2.6+1.1+3.2}_{-2.9-2.0-3.6})^\circ = (66.6^{+4.3}_{-5.0})^\circ, \\ d &= 0.410^{+0.053+0.001+0.010}_{-0.060-0.003-0.009} = 0.410^{+0.054}_{-0.061}, \\ \theta &= (155.9^{+2.5+10.8+0.8}_{-3.8-2.1-1.2})^\circ = (155.9^{+11.1}_{-4.5})^\circ, \end{aligned} \quad (2.15)$$

Here we show the errors arising from  $K$ ,  $\mathcal{A}_{\text{CP}}^{\text{dir}}(B_d \rightarrow \pi^+\pi^-)$  and  $\mathcal{A}_{\text{CP}}^{\text{mix}}(B_d \rightarrow \pi^+\pi^-)$ , and have finally added them in quadrature.



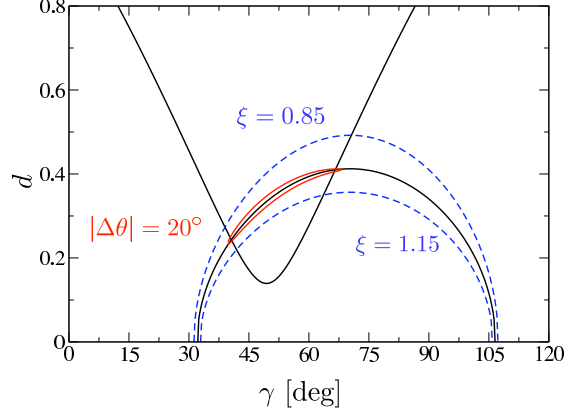


Figure 4: Illustration of the impact of  $U$ -spin-breaking corrections in the  $\gamma$ - $d$  plane.

## 2.4 Impact of $U$ -Spin-Breaking Effects

Let us now explore the impact of non-factorizable  $U$ -spin-breaking corrections to (2.7) by introducing the following parameters [21, 22]:

$$\xi \equiv d'/d, \quad \Delta\theta \equiv \theta' - \theta. \quad (2.16)$$

The expression for  $K$  in (2.10) is then modified as

$$K = \frac{1}{\epsilon^2} \left[ \frac{\epsilon^2 + 2\epsilon\xi d \cos(\theta + \Delta\theta) \cos \gamma + \xi^2 d^2}{1 - 2d \cos \theta \cos \gamma + d^2} \right]. \quad (2.17)$$

Since the numerator is governed by the  $\xi^2 d^2$  term, the dominant  $U$ -spin-breaking effects are described by  $\xi$ , whereas  $\Delta\theta$  plays a very minor rôle, as was also noted in Refs. [21, 22]. This behaviour can nicely be seen in Fig. 4, where we have considered  $\xi = 1 \pm 0.15$  and  $\Delta\theta = \pm 20^\circ$ . In view of the comments given above, these parameters describe generous  $U$ -spin-breaking effects. Their impact on the numerical solutions in (2.14) and (2.15) is given as follows:

$$\begin{aligned} \gamma &= (40.6^{+3.0+1.3+0.2}_{-2.8-1.6-0.3})^\circ, \\ d &= 0.243^{+0.028+0.030+0.006}_{-0.029-0.023-0.003}, \\ \theta &= (29.2^{+15.3+4.5+0.5}_{-13.3-4.3-0.8})^\circ, \end{aligned} \quad (2.18)$$

$$\begin{aligned} \gamma &= (66.6^{+4.3+4.0+0.1}_{-5.0-3.0-0.2})^\circ, \\ d &= 0.410^{+0.054+0.082+0.002}_{-0.061-0.060-0.001}, \\ \theta &= (155.9^{+11.1+3.6+0.1}_{-4.5-3.8-0.3})^\circ, \end{aligned} \quad (2.19)$$

where the second and third errors refer to  $\xi$  and  $\Delta\theta$ , respectively. Interestingly,  $\gamma$  is only moderately affected by these effects, which do not exceed the current experimental uncertainties for the parameter ranges considered above. Performing measurements of CP violation in  $B_s \rightarrow K^+ K^-$ , which will be possible with impressive accuracy at the LHCb experiment [23], the use of the  $U$ -spin symmetry can be minimized in the extraction of  $\gamma$ , and internal consistency checks become available. Before turning to these asymmetries, let us first discuss the discrete ambiguities affecting the extraction of  $\gamma$ .

## 2.5 Discrete Ambiguities

So far, we have restricted the discussion to the range of  $0^\circ \leq \gamma \leq 180^\circ$ , which follows from the SM interpretation of the measurement of  $\varepsilon_K$ , which describes the indirect CP violation in the neutral kaon system [24, 25]. However, if we allow for new physics (NP), we have to consider the whole range of  $\gamma$ . As can be seen by having a closer look at the expressions given in (2.2), (2.3) and (2.10), for each of the two solutions listed in (2.18) and (2.19), we obtain an additional one through the following transformation:

$$\gamma \rightarrow \gamma - 180^\circ, \quad d \rightarrow d, \quad \theta \rightarrow \theta - 180^\circ, \quad (2.20)$$

i.e. we have to deal with a fourfold discrete ambiguity, which has to be resolved for the search of NP.

To this end, let us first have a look at  $\cos \theta$  for (2.18) and (2.19), given by

$$\cos \theta = +0.873_{-0.168}^{+0.092} \quad \text{and} \quad \cos \theta = -0.913_{-0.064}^{+0.047}, \quad (2.21)$$

respectively, where we have added all errors in quadrature. Although non-factorizable effects have a significant impact on  $\theta$ , we do *not* expect that they will change the sign of the cosine of this strong phase, which is *negative* in the notation used above. Consequently, (2.18) can be excluded through this argument. As we will see in Subsection 2.6, the future measurement of mixing-induced CP violation in  $B_s \rightarrow K^+ K^-$  should allow us to rule out this solution in a *direct* way. Moreover, as will be discussed in Subsection 3.4, already the current data for the observables of the  $B_d \rightarrow \pi^\mp K^\pm$ ,  $B^\pm \rightarrow \pi^\pm K$  system exclude (2.18) and its “mirror” solution around  $\gamma = -139^\circ$  following from (2.20), where the sign of  $\cos \theta$  would be as in factorization. In the case of the remaining mirror solution of (2.19) around  $\gamma = -113^\circ$ , the sign of  $\cos \theta$  would be positive, i.e. opposite to our expectation, so that it can be ruled out as well.

Consequently, we are finally left with the numbers in (2.19). It is interesting to note that the corresponding value of  $\gamma$  in is in excellent agreement with the SM fits of the UT obtained by the UTfit and CKMfitter collaborations [24, 25], yielding  $\gamma = (64.6 \pm 4.2)^\circ$  and  $\gamma = (59.0_{-3.7}^{+9.2})^\circ$ , respectively.

## 2.6 CP Violation in $B_s \rightarrow K^+ K^-$

Using the expression for the  $B_s^0 \rightarrow K^+ K^-$  decay amplitude in (2.5), the observables entering the CP-violating rate asymmetry in (1.1) take the following form:

$$\mathcal{A}_{\text{CP}}^{\text{dir}}(B_s \rightarrow K^+ K^-) = \frac{2\epsilon d' \sin \theta' \sin \gamma}{d'^2 + 2\epsilon d' \cos \theta' \cos \gamma + \epsilon^2}, \quad (2.22)$$

$$\mathcal{A}_{\text{CP}}^{\text{mix}}(B_s \rightarrow K^+ K^-) = + \left[ \frac{d'^2 \sin \phi_s + 2\epsilon d' \cos \theta' \sin(\phi_s + \gamma) + \epsilon^2 \sin(\phi_s + 2\gamma)}{d'^2 + 2\epsilon d' \cos \theta' \cos \gamma + \epsilon^2} \right], \quad (2.23)$$

$$\mathcal{A}_{\Delta\Gamma}(B_s \rightarrow K^+ K^-) = - \left[ \frac{d'^2 \cos \phi_s + 2\epsilon d' \cos \theta' \cos(\phi_s + \gamma) + \epsilon^2 \cos(\phi_s + 2\gamma)}{d'^2 + 2\epsilon d' \cos \theta' \cos \gamma + \epsilon^2 d'^2} \right], \quad (2.24)$$

where  $\phi_s$  is the CP-violating  $B_s^0$ - $\bar{B}_s^0$  mixing phase; in the SM, it is given in terms of the Wolfenstein parameters by  $\phi_s = -2\lambda^2\eta$ , and takes a tiny value of  $\phi_s|_{\text{SM}} \approx -2^\circ$ . If we

consider this SM case for the solution of (2.15) and use the  $U$ -spin relations in (2.7), we arrive at the following predictions:

$$\begin{aligned}\mathcal{A}_{\text{CP}}^{\text{dir}}(B_s \rightarrow K^+ K^-) &= +0.101_{-0.020-0.043-0.000}^{+0.034+0.043+0.000} = +0.101_{-0.047}^{+0.055}, \\ \mathcal{A}_{\text{CP}}^{\text{mix}}(B_s \rightarrow K^+ K^-) &= -0.246_{-0.023-0.017-0.010}^{+0.018+0.029+0.012} = -0.246_{-0.030}^{+0.036}, \\ \mathcal{A}_{\Delta\Gamma}(B_s \rightarrow K^+ K^-) &= -0.964_{-0.006-0.002-0.003}^{+0.010+0.001+0.003} = -0.964_{-0.007}^{+0.011},\end{aligned}\quad (2.25)$$

where the treatment and notation of the errors is as in (2.14) and (2.15), i.e. refers to the uncertainties of  $K$ ,  $\mathcal{A}_{\text{CP}}^{\text{dir}}(B_d \rightarrow \pi^+ \pi^-)$  and  $\mathcal{A}_{\text{CP}}^{\text{mix}}(B_d \rightarrow \pi^+ \pi^-)$ . The interesting feature that the error of the direct CP asymmetry is independent of that of  $\mathcal{A}_{\text{CP}}^{\text{mix}}(B_d \rightarrow \pi^+ \pi^-)$  is due to the following  $U$ -spin relation [1]:

$$\mathcal{A}_{\text{CP}}^{\text{dir}}(B_s \rightarrow K^+ K^-) = -\frac{1}{\epsilon_K} \mathcal{A}_{\text{CP}}^{\text{dir}}(B_d \rightarrow \pi^+ \pi^-), \quad (2.26)$$

and provides a nice numerical test. Moreover, all observables satisfy the relation

$$[\mathcal{A}_{\text{CP}}^{\text{dir}}(B_s \rightarrow K^+ K^-)]^2 + [\mathcal{A}_{\text{CP}}^{\text{mix}}(B_s \rightarrow K^+ K^-)]^2 + [\mathcal{A}_{\Delta\Gamma}(B_s \rightarrow K^+ K^-)]^2 = 1. \quad (2.27)$$

The impact of the  $U$ -spin-breaking corrections discussed in Subsection 2.4 is given as follows:

$$\begin{aligned}\mathcal{A}_{\text{CP}}^{\text{dir}}(B_s \rightarrow K^+ K^-) &= +0.101_{-0.047-0.015-0.083}^{+0.055+0.015+0.067}, \\ \mathcal{A}_{\text{CP}}^{\text{mix}}(B_s \rightarrow K^+ K^-) &= -0.246_{-0.030-0.007-0.023}^{+0.036+0.008+0.051}, \\ \mathcal{A}_{\Delta\Gamma}(B_s \rightarrow K^+ K^-) &= -0.964_{-0.007-0.000-0.002}^{+0.011+0.000+0.001},\end{aligned}\quad (2.28)$$

where the second and third errors refer to  $\xi = 1 \pm 0.15$  and  $\Delta\theta = \pm 20^\circ$ , respectively, as in (2.18) and (2.19). Whereas  $\mathcal{A}_{\text{CP}}^{\text{mix}}(B_s \rightarrow K^+ K^-)$  and  $\mathcal{A}_{\Delta\Gamma}(B_s \rightarrow K^+ K^-)$  are pretty stable with respect to the  $U$ -spin-breaking effects, the direct CP asymmetry is significantly affected by  $\Delta\theta$ . As we will discuss in Subsection 3.4, the measurement of the direct CP violation in  $B_d \rightarrow \pi^\mp K^\pm$  strongly disfavors such effects.

The next important step in the analysis of the  $B_d \rightarrow \pi^+ \pi^-$ ,  $B_s \rightarrow K^+ K^-$  system is the measurement of the mixing-induced CP violation in  $B_s^0 \rightarrow K^+ K^-$ . Applying the formulae given in Ref. [1], this observable can be combined with  $K$  to fix another contour in the  $\gamma$ - $d$  plane. In Fig. 5, we illustrate the corresponding situation for the central numerical values given above, and observe that the measurement of  $\mathcal{A}_{\text{CP}}^{\text{mix}}(B_s \rightarrow K^+ K^-)$  will in fact allow us to resolve the twofold ambiguity in the extraction of the UT angle  $\gamma$ , as we noted in Subsection 2.5.

Finally, if also the direct CP asymmetry  $\mathcal{A}_{\text{CP}}^{\text{dir}}(B_s \rightarrow K^+ K^-)$  is measured, we can combine it with  $\mathcal{A}_{\text{CP}}^{\text{mix}}(B_s \rightarrow K^+ K^-)$  to calculate  $d'$  as a function of  $\gamma$  for a given value of the mixing phase  $\phi_s$  [1]. It should be emphasized that this contour is – in contrast to those involving  $K$  – *theoretically clean*, in analogy to the  $\gamma$ - $d$  curve following from the CP-violating  $B_d \rightarrow \pi^+ \pi^-$  observables. Using the first of the  $U$ -spin relations in (2.7), we can then extract  $\gamma$  and  $d$ , where the information provided by  $K$  allows us to resolve the discrete ambiguity. Since the strong phases  $\theta$  and  $\theta'$  can be determined as well, we may actually perform a test of the second  $U$ -spin relation in (2.7). Moreover, the impact of  $U$ -spin-breaking corrections to  $d' = d$  corresponds to a relative shift of the  $B_d \rightarrow \pi^+ \pi^-$  and  $B_s \rightarrow K^+ K^-$  contours; the situation for the extraction of  $\gamma$  in Fig. 5 would actually be very stable in this respect. This would be the most refined implementation of the

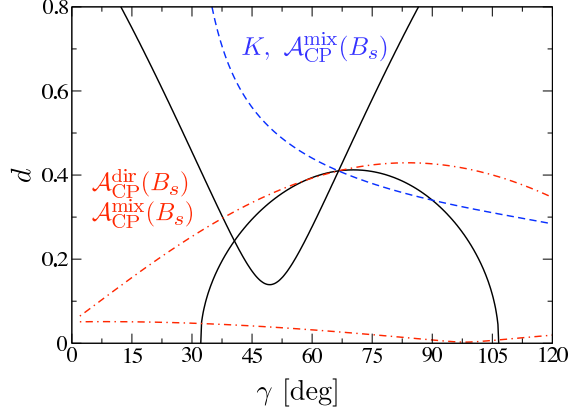


Figure 5: Illustration of the impact of the measurement of the CP-violating observables of the  $B_s^0 \rightarrow K^+K^-$  decay on the situation in the  $\gamma$ - $d$  plane within the SM.

$B_s \rightarrow K^+K^-$ ,  $B_d \rightarrow \pi^+\pi^-$  strategy for the extraction of  $\gamma$ . For recent LHCb studies, which look very promising, see Ref. [23].

The last observable that is provided by  $B_s^0 \rightarrow K^+K^-$  is  $\mathcal{A}_{\Delta\Gamma}(B_s \rightarrow K^+K^-)$ , which enters the following “untagged” rate [26]:

$$\begin{aligned} \langle \Gamma(B_s(t) \rightarrow K^+K^-) \rangle &\equiv \Gamma(B_s^0(t) \rightarrow K^+K^-) + \Gamma(\bar{B}_s^0(t) \rightarrow K^+K^-) \\ &\propto e^{-\Gamma_s t} [e^{+\Delta\Gamma_s t/2} R_L(B_s \rightarrow K^+K^-) + e^{-\Delta\Gamma_s t/2} R_H(B_s \rightarrow K^+K^-)], \end{aligned} \quad (2.29)$$

where

$$\Gamma_s \equiv \frac{\Gamma_H^{(s)} + \Gamma_L^{(s)}}{2}, \quad \Delta\Gamma_s \equiv \Gamma_H^{(s)} - \Gamma_L^{(s)} \quad (2.30)$$

depend on the decay widths  $\Gamma_H^{(s)}$  and  $\Gamma_L^{(s)}$  of the “heavy” and “light” mass eigenstates of the  $B_s$  system, respectively, and

$$R_L(B_s \rightarrow K^+K^-) \equiv 1 - \mathcal{A}_{\Delta\Gamma}(B_s \rightarrow K^+K^-) = 1.964_{-0.011}^{+0.007}, \quad (2.31)$$

$$R_H(B_s \rightarrow K^+K^-) \equiv 1 + \mathcal{A}_{\Delta\Gamma}(B_s \rightarrow K^+K^-) = 0.036_{-0.007}^{+0.011}; \quad (2.32)$$

the numerical values correspond to the SM prediction in (2.28). Concerning a practical measurement of (2.29), most data come from short times with  $\Delta\Gamma_s t \ll 1$ :

$$\langle \Gamma(B_s(t) \rightarrow K^+K^-) \rangle \propto e^{-\Gamma_s t} \left[ 1 - \mathcal{A}_{\Delta\Gamma}(B_s \rightarrow K^+K^-) \left( \frac{\Delta\Gamma_s t}{2} \right) + \mathcal{O}((\Delta\Gamma_s t)^2) \right]. \quad (2.33)$$

Moreover, if the two-exponential form of (2.29) is fitted to a single exponential, the corresponding decay width satisfies the following relation [27]:

$$\Gamma_{K^+K^-} = \Gamma_s + \mathcal{A}_{\Delta\Gamma}(B_s \rightarrow K^+K^-) \frac{\Delta\Gamma_s}{2} + \mathcal{O}((\Delta\Gamma_s)^2/\Gamma_s). \quad (2.34)$$

First studies along these lines were recently performed by the CDF collaboration [28], yielding  $\tau(B_s \rightarrow K^+K^-) = 1/\Gamma_{K^+K^-} = (1.53 \pm 0.18 \pm 0.02)$  ps. Using flavour-specific  $B_s$  decays, a similar analysis allows the extraction of  $\Gamma_s$  up to corrections of  $\mathcal{O}((\Delta\Gamma_s/\Gamma_s)^2)$  [27]. With the help of the analysis discussed above, which allows the calculation of  $\mathcal{A}_{\Delta\Gamma}(B_s \rightarrow K^+K^-)$ , the width difference  $\Delta\Gamma_s$  can then be extracted.

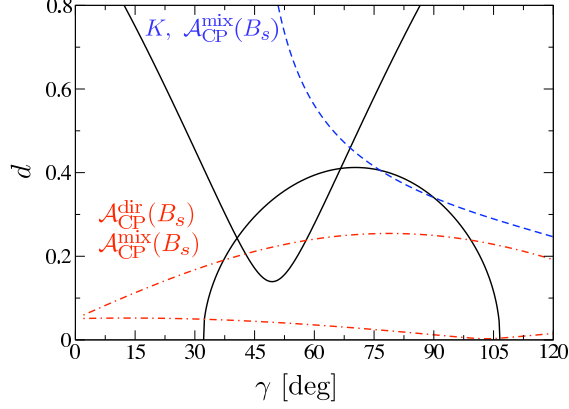


Figure 6: Illustration of the impact of CP-violating NP contributions to  $B_s^0\text{--}\bar{B}_s^0$  mixing leading to  $\phi_s = -10^\circ$  on the contours in the  $\gamma$ – $d$  plane.

## 2.7 Impact of New Physics

Because of the impressive agreement of the value of  $\gamma$  that we extracted from the  $B_d \rightarrow \pi^+\pi^-$ ,  $B_s \rightarrow K^+K^-$  data with the fits of the UT and the overall consistency with the SM (see also Section 3), dramatic NP contributions to the corresponding decay amplitudes are already excluded, although the experimental picture has still to be improved considerably. In particular, accurate measurements of  $\gamma$  through pure tree-level decays are not yet available, but will be performed at LHCb [14]; important examples are  $B_s \rightarrow D_s^\pm K^\mp$  and  $B_d \rightarrow D^\pm \pi^\mp$  decays, where the  $U$ -spin symmetry provides again a useful tool [29].

Similar conclusions about NP effects in  $B \rightarrow \pi\pi, \pi K$  modes were drawn in Refs. [10, 30]. The corresponding  $B$ -factory data may indicate a modified EW penguin sector with a large CP-violating NP phase through the results for mixing-induced CP violation in  $B_d^0 \rightarrow \pi^0 K_S$ , thereby complementing the pattern of such CP asymmetries observed in other  $b \rightarrow s$  penguin modes, where the  $B_d^0 \rightarrow \phi K_S$  channel is an outstanding example. Since EW penguin topologies contribute to the  $B_s \rightarrow K^+K^-$ ,  $B_d \rightarrow \pi^+\pi^-$  (and the  $B_d \rightarrow \pi^\mp K^\pm$ ,  $B_s \rightarrow \pi^\pm K^\mp$ ) system in colour-suppressed form, they play there a minor rôle. Consequently, NP effects entering through the EW penguin sector could not be seen in the analysis discussed in this paper.

On the other hand,  $B_s^0\text{--}\bar{B}_s^0$  mixing offers a nice avenue for NP to manifest itself in  $B_s^0 \rightarrow K^+K^-$ . The mass difference  $\Delta M_s$  was recently measured at the Tevatron [31, 32], with a value that is consistent with the SM expectation. On the other hand, this result still allows for large CP-violating NP contributions to  $B_s^0\text{--}\bar{B}_s^0$  mixing (see, for instance, Refs. [33, 34]). In this case, the mixing phase  $\phi_s$ , which can be extracted through the time-dependent angular distribution of the  $B_s^0 \rightarrow J/\psi[\rightarrow \mu^+\mu^-]\phi[\rightarrow K^+K^-]$  decay products [27, 35], would take a sizeable value. Interestingly, also the  $B_s \rightarrow K^+K^-$ ,  $B_d \rightarrow \pi^+\pi^-$  system allows us to search for NP effects of this kind. Assuming a value of  $\phi_s = -10^\circ$ , which corresponds to a simple “translation” of the tension in the CKM fits between  $(\sin 2\beta)_{\psi K_S}$  and the UT side  $R_b \propto |V_{ub}/V_{cb}|$  [33], we arrive at the situation illustrated in Fig. 6. There we show the contours involving  $\mathcal{A}_{\text{CP}}^{\text{mix}}(B_s \rightarrow K^+K^-)$  that would arise if we assume the SM value of  $\phi_s$ . In this case, we would arrive at quite

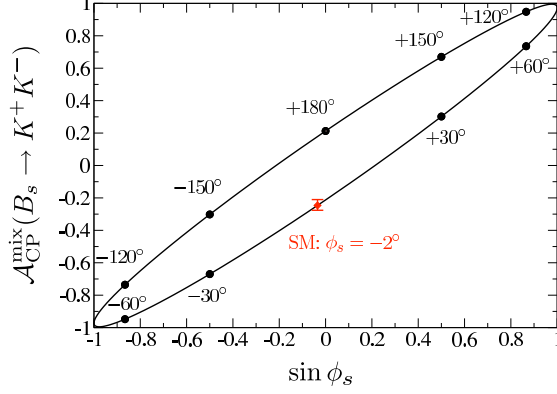


Figure 7: The correlation between  $\sin \phi_s$ , which can be determined through mixing-induced CP violation in  $B_s^0 \rightarrow J/\psi \phi$ , and  $\mathcal{A}_{\text{CP}}^{\text{mix}}(B_s \rightarrow K^+ K^-)$  for the central values of the parameters in (2.15); in the SM case, we show also the error bar. Each point on the curve corresponds to a given value of  $\phi_s$ , as indicated by the numerical values.

some discrepancy, in particular through the contour following from the CP-violating  $B_s \rightarrow K^+ K^-$  asymmetries. For larger values of  $\phi_s$ , the discrepancy would be even more pronounced. In this case, the measured value of  $\mathcal{A}_{\text{CP}}^{\text{mix}}(B_s \rightarrow K^+ K^-)$  would also not lie on the SM surface in observable space that was calculated in Ref. [36].

It is instructive to expand (2.23) and (2.24) in powers of  $\epsilon/d' \sim 0.1$ , yielding

$$\mathcal{A}_{\text{CP}}^{\text{mix}}(B_s \rightarrow K^+ K^-) = +\sin \phi_s + 2 \left( \frac{\epsilon}{d'} \right) \cos \theta' \sin \gamma \cos \phi_s + \mathcal{O}((\epsilon/d')^2), \quad (2.35)$$

$$\mathcal{A}_{\Delta\Gamma}(B_s \rightarrow K^+ K^-) = -\cos \phi_s + 2 \left( \frac{\epsilon}{d'} \right) \cos \theta' \sin \gamma \sin \phi_s + \mathcal{O}((\epsilon/d')^2), \quad (2.36)$$

where  $2(\epsilon/d') \cos \theta' \sin \gamma \approx -0.2$ . We observe two interesting features:

- $\mathcal{A}_{\text{CP}}^{\text{mix}}(B_s \rightarrow K^+ K^-)$  is strongly affected if  $\phi_s$  moves away from 0 thanks to the  $\sin \phi_s$  term, and offers also information on  $\cos \phi_s$  through the hadronic piece.
- $\mathcal{A}_{\Delta\Gamma}(B_s \rightarrow K^+ K^-)$  deviates slowly from its SM value around  $-1$  as  $\phi_s$  moves away from 0, and the hadronic term is suppressed by  $\sin \phi_s$  for small phases, which is the reason for the remarkably small uncertainty of the SM prediction in Subsection 2.6.

In Fig. 7, we show the correlation between  $\sin \phi_s$ , which is determined through the time-dependent angular analysis of the  $B_s^0 \rightarrow J/\psi[\rightarrow \mu^+ \mu^-] \phi[\rightarrow K^+ K^-]$  decay products [35], and the mixing-induced CP violation in  $B_s^0 \rightarrow K^+ K^-$ , which can be predicted with the help of the parameters in (2.15). This figure shows nicely that the combination of both observables allows an *unambiguous* determination of  $\phi_s$ . In particular, we may also distinguish between the cases of  $\phi_s = 0^\circ$  and  $180^\circ$ , which is important for the search of NP. Recently, the D0 collaboration has reported first results for the measurement of  $\phi_s$  through an *untagged*  $B_s^0 \rightarrow J/\psi \phi$  analysis [37], which suffers from a four-fold discrete ambiguity. The solution closest to the SM case reads as

$$\phi_s = -0.79 \pm 0.56 (\text{stat.})^{+0.14}_{-0.01} (\text{syst.}) = -(45 \pm 32^{+1}_{-8})^\circ, \quad (2.37)$$

so that this quantity is still largely unconstrained.

Let us finally come back to the untagged rate in (2.33). In the presence of NP,  $\Delta\Gamma_s$  is modified as follows [38]:

$$\Delta\Gamma_s = \Delta\Gamma_s^{\text{SM}} \cos \phi_s, \quad (2.38)$$

where  $\Delta\Gamma_s^{\text{SM}}/\Gamma_s$  is negative for the definition in (2.30), and calculated at the 15% level [39]. Consequently, NP effects can only reduce the value of  $|\Delta\Gamma_s|$ . If  $\phi_s$  is determined as described above, the calculation of  $\mathcal{A}_{\Delta\Gamma}(B_s \rightarrow K^+ K^-)$  through the  $B_s \rightarrow K^+ K^-$ ,  $B_d \rightarrow \pi^+ \pi^-$  analysis allows the extraction of  $\Delta\Gamma_s^{\text{SM}}$  from the  $\tau(B_s \rightarrow K^+ K^-)$  lifetime, thereby complementing the extraction of this width difference through the  $B_s \rightarrow J/\psi \phi$  angular analysis [35].

### 3 The $B_d \rightarrow \pi^\mp K^\pm$ , $B_s \rightarrow \pi^\pm K^\mp$ Strategy

#### 3.1 First Insights into $U$ -Spin-Breaking Effects

Let us now discuss the  $U$ -spin-related decays  $B_d^0 \rightarrow \pi^- K^+$  and  $B_s^0 \rightarrow \pi^+ K^-$  [5]. If we use the unitarity of the CKM matrix, their decay amplitudes can be written as follows:

$$A(B_d^0 \rightarrow \pi^- K^+) = -P [1 - r e^{i\delta} e^{i\gamma}], \quad (3.1)$$

$$A(B_s^0 \rightarrow \pi^+ K^-) = P_s \sqrt{\epsilon} \left[ 1 + \frac{1}{\epsilon} r_s e^{i\delta_s} e^{i\gamma} \right], \quad (3.2)$$

where  $P_{(s)}$  and  $r_{(s)} e^{i\delta_{(s)}}$  are CP-conserving hadronic parameters, which describe penguin amplitudes and the ratio of trees to penguins, respectively. Using the  $U$ -spin flavour symmetry of strong interactions, we obtain – in analogy to (2.7) – the following relations:

$$r_s = r, \quad \delta_s = \delta. \quad (3.3)$$

In the case of the relation between  $|P_s|$  and  $|P|$ , factorizable  $U$ -spin-breaking corrections arise, which are described by the following ratio of decay constants and form factors:

$$\left| \frac{P_s}{P} \right|_{\text{fact}} = \frac{f_\pi}{f_K} \frac{F_{B_s K}(M_\pi^2; 0^+)}{F_{B_d \pi}(M_K^2; 0^+)} \left( \frac{M_{B_s}^2 - M_K^2}{M_{B_d}^2 - M_\pi^2} \right). \quad (3.4)$$

Using the recent QCD sum-rule results of Ref. [20] yields

$$\left| \frac{P_s}{P} \right|_{\text{fact}}^{\text{QCDSR}} = 1.02_{-0.10}^{+0.11}. \quad (3.5)$$

At first sight, it appears as if  $\gamma$ ,  $r$  and  $\delta$  could be determined with the help of the  $U$ -spin symmetry from the ratio of the CP-averaged branching ratios and the two CP asymmetries provided by the  $B_d \rightarrow \pi^\mp K^\pm$ ,  $B_s \rightarrow \pi^\pm K^\mp$  system. However, because of the following  $U$ -spin relation, which is the counterpart of (2.26), this is actually not the case:

$$\frac{\mathcal{A}_{\text{CP}}^{\text{dir}}(B_s \rightarrow \pi^\pm K^\mp)}{\mathcal{A}_{\text{CP}}^{\text{dir}}(B_d \rightarrow \pi^\mp K^\pm)} = - \left| \frac{P_s}{P} \right|^2 \left[ \frac{M_{B_d}}{M_{B_s}} \frac{\Phi(M_\pi/M_{B_s}, M_K/M_{B_s})}{\Phi(M_\pi/M_{B_d}, M_K/M_{B_d})} \frac{\tau_{B_s}}{\tau_{B_d}} \right] \left[ \frac{\text{BR}(B_d \rightarrow \pi^\mp K^\pm)}{\text{BR}(B_s \rightarrow \pi^\pm K^\mp)} \right]. \quad (3.6)$$

On the other hand, it allows us to obtain experimental insights into  $U$ -spin-breaking effects with the help of the measurements of the CP asymmetries and the CP-averaged branching ratios listed in Section 1. Adding the errors in quadrature, we obtain

$$\left| \frac{P_s}{P} \right|_{\text{exp}} = \left| \frac{P_s}{P} \right| \sqrt{\left[ \frac{r_s}{r} \right] \left[ \frac{\sin \delta_s}{\sin \delta} \right]} = 1.06 \pm 0.28, \quad (3.7)$$

where we have also taken non-factorizable  $U$ -spin-breaking effects to (3.3) into account. We obtain excellent agreement with (3.5), although the experimental uncertainties are still large. This quantity should be closely monitored as the data improve, allowing us to obtain valuable insights into non-factorizable  $U$ -spin-breaking effects. We shall return to this issue below.

### 3.2 Further Information: $B^+ \rightarrow \pi^+ K^0$ and $B^+ \rightarrow K^+ \bar{K}^0$

For the determination of  $\gamma$  from the  $B_d \rightarrow \pi^\mp K^\pm$ ,  $B_s \rightarrow \pi^\pm K^\mp$  system, the overall normalization  $P$  has to be fixed through an additional input, which is offered by the decay  $B^+ \rightarrow \pi^+ K^0$ . If we neglect colour-suppressed EW penguin topologies and use the  $SU(2)$  isospin symmetry of strong interactions, we may write its amplitude as follows:

$$A(B^+ \rightarrow \pi^+ K^0) = P [1 + \epsilon \rho_{\pi K} e^{i\theta_{\pi K}} e^{i\gamma}], \quad (3.8)$$

where the CP-conserving hadronic parameter  $\rho_{\pi K} e^{i\theta_{\pi K}}$  is expected to play a minor rôle because of the  $\epsilon$  suppression. A first probe of this quantity is offered by the direct CP asymmetry

$$\mathcal{A}_{\text{CP}}^{\text{dir}}(B^\pm \rightarrow \pi^\pm K) = - \left[ \frac{2\epsilon \rho_{\pi K} \sin \theta_{\pi K} \sin \gamma}{1 + 2\epsilon \rho_{\pi K} \cos \theta_{\pi K} \cos \gamma + \epsilon^2 \rho_{\pi K}^2} \right] = -0.009 \pm 0.025. \quad (3.9)$$

The experimental value [6], which is the average of the corresponding  $B$ -factory results, does not indicate any anomalous enhancement of  $\rho_{\pi K} e^{i\theta_{\pi K}}$ . This parameter can actually be determined with the help of the  $U$ -spin-related decay  $B^+ \rightarrow K^+ \bar{K}^0$  [40, 41]. In the SM, its transition amplitude can be written as follows:

$$A(B^+ \rightarrow K^+ \bar{K}^0) = \sqrt{\epsilon} P_{KK} [1 - \rho_{KK} e^{i\theta_{KK}} e^{i\gamma}], \quad (3.10)$$

where the  $U$ -spin symmetry implies

$$\rho_{KK} = \rho_{\pi K}, \quad \theta_{KK} = \theta_{\pi K}. \quad (3.11)$$

This channel was recently discovered at the  $B$  factories with the following CP-averaged branching ratios:

$$\text{BR}(B^\pm \rightarrow K^\pm K) = \begin{cases} (1.61 \pm 0.44 \pm 0.09) \times 10^{-6} & (\text{BaBar}) [42] \\ (1.22^{+0.33+0.13}_{-0.28-0.16}) \times 10^{-6} & (\text{Belle}) [43], \end{cases} \quad (3.12)$$

which correspond to the average

$$\text{BR}(B^\pm \rightarrow K^\pm K) = (1.36^{+0.29}_{-0.27}) \times 10^{-6}. \quad (3.13)$$



Moreover, also a first result for the corresponding direct CP asymmetry is available:

$$\mathcal{A}_{\text{CP}}^{\text{dir}}(B^\pm \rightarrow K^\pm K) = \frac{2\rho_{KK} \sin \theta_{KK} \sin \gamma}{1 - 2\rho_{KK} \cos \theta_{KK} \cos \gamma + \rho_{KK}^2} = -0.12_{-0.17}^{+0.18}. \quad (3.14)$$

The branching ratios are interestingly measured close to lower bounds that can be derived in the SM [44]. In fact, if we introduce

$$H_{\pi K}^{KK} \equiv \frac{1}{\epsilon} \left| \frac{P}{P_{KK}} \right|^2 \left[ \frac{\Phi(M_\pi/M_B, M_K/M_B)}{\Phi(M_K/M_B, M_K/M_B)} \right] \left[ \frac{\text{BR}(B^\pm \rightarrow K^\pm K)}{\text{BR}(B^\pm \rightarrow \pi^\pm K)} \right], \quad (3.15)$$

we obtain

$$H_{\pi K}^{KK} = \frac{1 - 2\rho_{KK} \cos \theta_{KK} \cos \gamma + \rho_{KK}^2}{1 + 2\epsilon \rho_{\pi K} \cos \theta_{\pi K} \cos \gamma + \epsilon^2 \rho_{\pi K}^2}. \quad (3.16)$$

This quantity takes the following lower bound:

$$H_{\pi K}^{KK} \geq [1 - 2\epsilon \cos^2 \gamma + \mathcal{O}(\epsilon^2)] \sin^2 \gamma, \quad (3.17)$$

which can be converted into a lower bound for  $\text{BR}(B^\pm \rightarrow K^\pm K)$  with the help of the measured  $B^\pm \rightarrow \pi^\pm K$  branching ratio. Moreover, also the  $U$ -spin-breaking corrections to  $|P/P_{KK}|$  have to be determined. In the factorization approximation, we have

$$\left| \frac{P_{KK}}{P} \right|_{\text{fact}} = \frac{F_{BK}(M_K^2; 0^+)}{F_{B\pi}(M_K^2; 0^+)} \left( \frac{M_B^2 - M_K^2}{M_B^2 - M_\pi^2} \right). \quad (3.18)$$

Using once again the QCD sum-rule results of Ref. [20] yields

$$\left| \frac{P_{KK}}{P} \right|_{\text{fact}}^{\text{QCDSR}} = 1.35_{-0.09}^{+0.11}, \quad (3.19)$$

which agrees with an alternative analysis [45]. The experimental branching ratio in (1.4) and the result for  $\gamma$  in (2.15) yield then the following lower bound:

$$\text{BR}(B^\pm \rightarrow K^\pm K)_{\text{min}} = (1.78_{-0.26}^{+0.23}) \times 10^{-6}, \quad (3.20)$$

where all errors were again added in quadrature. While the BaBar result in (3.12) is fully consistent with this bound, the Belle measurement is clearly on the lower side, and reduces also the average in (3.13), which yields

$$H_{\pi K}^{KK} = 0.64 \pm 0.15. \quad (3.21)$$

Using (3.17), this value can be converted into the following upper bound on  $\gamma$ :

$$\gamma \leq (53_{-9}^{+10})^\circ. \quad (3.22)$$

It is about  $1\sigma$  below the result for  $\gamma$  in (2.15), which is another manifestation of the low branching ratio in (3.13).

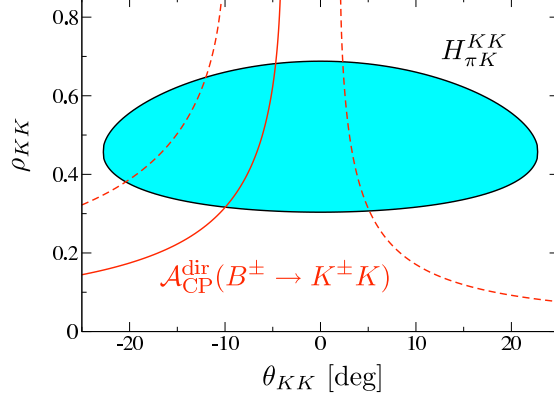


Figure 8: The constraints in the  $\theta_{KK}$ - $\rho_{KK}$  plane following from  $H_{\pi K}^{KK}$  and  $\mathcal{A}_{\text{CP}}^{\text{dir}}(B^\pm \rightarrow K^\pm K)$ , as explained in the text ( $\gamma = 61.6^\circ$ ,  $H_{\pi K}^{KK} = 0.79$ ).

For a given value of  $\gamma$ , (3.16) allows us to calculate  $\rho_{KK}$  as a function of  $\theta_{KK}$  with the help of the  $U$ -spin relations in (3.11):

$$\rho_{KK} = a \pm \sqrt{a^2 - b}, \quad (3.23)$$

where

$$a = \left[ \frac{1 + \epsilon H_{\pi K}^{KK}}{1 - \epsilon^2 H_{\pi K}^{KK}} \right] \cos \theta_{KK} \cos \gamma, \quad b = \frac{1 - H_{\pi K}^{KK}}{1 - \epsilon^2 H_{\pi K}^{KK}}. \quad (3.24)$$

Another contour can be fixed through the direct CP asymmetry in (3.14). To this end, we have just to make the following replacements in (3.23):

$$a \rightarrow \cos \gamma \cos \theta_{KK} + \frac{\sin \gamma \sin \theta_{KK}}{\mathcal{A}_{\text{CP}}^{\text{dir}}(B^\pm \rightarrow K^\pm K)}, \quad b \rightarrow 1. \quad (3.25)$$

It should be emphasized that this curve is valid exactly, i.e. does not rely on the  $U$ -spin symmetry. Because of the bounds discussed above, (3.23) with (3.24) does not give physical solutions for the central values of  $\gamma = 66.6^\circ$  and  $H_{\pi K}^{KK} = 0.64$ . However, if we lower  $\gamma$  by one sigma to  $61.6^\circ$  and increase  $H_{\pi K}^{KK}$  by one sigma to 0.79, we arrive at the situation shown in Fig. 8, leaving us with a pretty constrained allowed region around

$$\rho_{KK} \approx \rho_{\pi K} \sim 0.5, \quad \theta_{KK} \approx \theta_{\pi K} \sim 0^\circ. \quad (3.26)$$

Consequently, we find  $\epsilon \rho_{\pi K}|_{\text{exp}} \sim 0.025$ , so that we do not have to worry about the effects of this parameter. In toy models of final-state interaction effects that were considered several years ago, this parameter would have been enhanced by up to one order of magnitude. These scenarios are therefore ruled out by the  $B$ -factory data. Moreover, anomalous enhancements of colour-suppressed EW penguin contributions, which would arise in such scenarios as well, are also disfavoured.

### 3.3 Extracting the UT Angle $\gamma$

Let us first have a look at the  $B_d \rightarrow \pi^\mp K^\pm$ ,  $B^\pm \rightarrow \pi^\pm K$  system. For the extraction of  $\gamma$ , we introduce the following ratio [46]:

$$R \equiv \left[ \frac{M_{B_d}}{M_{B^+}} \frac{\Phi(M_\pi/M_{B^+}, M_K/M_{B^+})}{\Phi(M_\pi/M_{B_d}, M_K/M_{B_d})} \frac{\tau_{B^+}}{\tau_{B_d}} \right] \left[ \frac{\text{BR}(B_d \rightarrow \pi^\mp K^\pm)}{\text{BR}(B^\pm \rightarrow \pi^\pm K)} \right] = 0.899 \pm 0.049, \quad (3.27)$$

where we have included tiny phase-space effects, used  $\tau_{B^+}/\tau_{B_d^0} = 1.071 \pm 0.009$  [47], and added the errors in quadrature. The amplitude parametrizations in (3.1) and (3.8) imply then the following expression [41]:

$$w^2 R = 1 - 2r \cos \delta \cos \gamma + r^2, \quad (3.28)$$

with

$$w = \sqrt{1 + 2\epsilon \rho_{\pi K} \cos \theta_{\pi K} + \epsilon^2 \rho_{\pi K}^2}. \quad (3.29)$$

Using (3.26), we obtain  $w^2 \sim 1.02$ . The corresponding effect lies within the errors of (3.27) and will be neglected in the following discussion. Following Ref. [46], where the bound

$$\sin^2 \gamma \leq R \quad (3.30)$$

was derived, we obtain

$$\gamma \leq (71.5^{+5.3}_{-4.3})^\circ, \quad (3.31)$$

where the errors reflect the uncertainties of  $R$ . The value of  $\gamma$  in (2.15) and the SM fits of the UT are well consistent with this bound, which effectively constrains  $\gamma$  in a phenomenologically very interesting region.

If we combine  $R$  with the direct CP asymmetry of  $B_d^0 \rightarrow \pi^- K^+$ , the strong phase  $\delta$  can be eliminated, allowing us to calculate  $r$  as a function of  $\gamma$ . To this end, it is convenient to introduce the following ‘‘pseudo-asymmetry’’ [48]:

$$A_0 \equiv \mathcal{A}_{\text{CP}}^{\text{dir}}(B_d \rightarrow \pi^\mp K^\pm) R = 2r \sin \delta \sin \gamma, \quad (3.32)$$

so that

$$r = \sqrt{a_d \pm \sqrt{a_d^2 - b_d}}, \quad (3.33)$$

with

$$a_d = R - \sin^2 \gamma + \cos^2 \gamma, \quad (3.34)$$

$$b_d = (1 - R)^2 + \left( \frac{A_0 \cos \gamma}{\sin \gamma} \right)^2; \quad (3.35)$$

for generalized expressions, taking also the effects of  $(\rho_{\pi K}, \theta_{\pi K})$  and colour-suppressed EW penguins into account, see Ref. [41]. For given values of  $\gamma$  and  $r$ , the strong phase  $\delta$  can unambiguously be determined through

$$r \cos \delta = \cos \gamma \pm \text{sgn}(\cos \gamma) \sqrt{\cos^2 \gamma - (1 - R) - \left( \frac{A_0}{2 \sin \gamma} \right)^2}, \quad (3.36)$$

$$r \sin \delta = \frac{A_0}{2 \sin \gamma}. \quad (3.37)$$

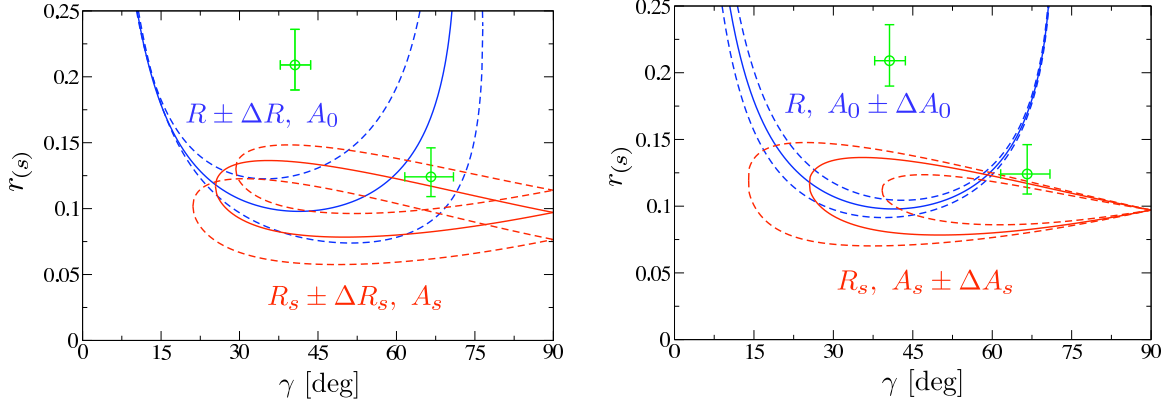


Figure 9: The contours in the  $\gamma$ - $r_{(s)}$  plane: the left panel shows the  $1\sigma$  ranges of the  $R_{(s)}$  (upper and lower curves correspond to  $R_{(s)} + \Delta R_{(s)}$  and  $R_{(s)} - \Delta R_{(s)}$ , respectively), the right panel the  $1\sigma$  ranges of the corresponding direct CP asymmetries (upper and lower curves correspond to  $\mathcal{A}_{\text{CP}}^{\text{dir}} + \Delta \mathcal{A}_{\text{CP}}^{\text{dir}}$  and  $\mathcal{A}_{\text{CP}}^{\text{dir}} - \Delta \mathcal{A}_{\text{CP}}^{\text{dir}}$ , respectively). The error bars represent the results for  $\gamma$  and  $d$  in (2.14) and (2.15).

As  $R < 1$ , we have  $\text{sgn}(\cos \delta) = \text{sgn}(\cos \gamma)$  for the two solutions of  $r$ . Consequently, since we expect a positive value of the cosine of  $\delta$ , as in factorization, we are left with the range of  $-90^\circ < \gamma < +90^\circ$ . Since the four solutions for  $\gamma$  following from (2.14) and (2.15) with (2.20) overlap with that region only for  $0^\circ < \gamma < 90^\circ$ , we may restrict the following discussion to this range.

The determination of  $\gamma$  requires further information, which can be obtained with the help of the  $B_s^0 \rightarrow \pi^+ K^-$  channel. To this end, we introduce – in analogy to (3.27) and (3.32) – the following quantities:

$$R_s \equiv \left| \frac{P}{P_s} \right|^2 \left[ \frac{M_{B_s}}{M_{B^+}} \frac{\Phi(M_\pi/M_{B^+}, M_K/M_{B^+}) \tau_{B^+}}{\Phi(M_\pi/M_{B_s}, M_K/M_{B_s}) \tau_{B_s}} \right] \left[ \frac{\text{BR}(B_s \rightarrow \pi^\pm K^\mp)}{\text{BR}(B^\pm \rightarrow \pi^\pm K)} \right]$$

$$= \epsilon + 2r_s \cos \delta_s \cos \gamma + \frac{r_s^2}{\epsilon} = 0.236 \pm 0.070, \quad (3.38)$$

where (3.5) as well as  $\tau_{B^+} = (1.638 \pm 0.011)\text{ps}$  and  $\tau_{B_s} = (1.466 \pm 0.059)\text{ps}$  [47] enter the numerical value, and

$$A_s \equiv \mathcal{A}_{\text{CP}}^{\text{dir}}(B_s \rightarrow \pi^\pm K^\mp) R_s = -2r_s \sin \delta_s \sin \gamma. \quad (3.39)$$

These quantities allow us to eliminate the strong phase  $\delta_s$ , and to calculate  $r_s$  as a function of  $\gamma$ . To this end, we have simply to make the replacements  $r \rightarrow r_s$ ,  $a_d \rightarrow a_s$  and  $b_d \rightarrow b_s$  in (3.33), with

$$a_s = \epsilon [R_s - \epsilon (\sin^2 \gamma - \cos^2 \gamma)], \quad (3.40)$$

$$b_s = \epsilon^2 \left[ (R_s - \epsilon)^2 + \left( \frac{A_s \cos \gamma}{\sin \gamma} \right)^2 \right]. \quad (3.41)$$

For given values of  $\gamma$  and  $r_s$ , we may again extract the strong phase unambiguously with the help of the relations

$$r_s \cos \delta_s = -\epsilon \cos \gamma \mp \text{sgn}(\cos \gamma) \sqrt{\epsilon (R_s - \epsilon \sin^2 \gamma) - \left(\frac{A_s}{2 \sin \gamma}\right)^2}, \quad (3.42)$$

$$r_s \sin \delta_s = -\left(\frac{A_s}{2 \sin \gamma}\right). \quad (3.43)$$

Using, finally, the first  $U$ -spin relation given in (3.3), the intersection of the  $\gamma$ - $r$  and  $\gamma$ - $r_s$  contours allows the extraction of  $\gamma$  and  $r_s = r$ . Moreover, also the strong phases can be extracted, providing an internal consistency check of the  $U$ -spin symmetry;  $U$ -spin-breaking corrections to  $r_s = r$  correspond to a relative shift of both contours. In Fig. 9, we show these curves for the current data, exploring also the impact of their uncertainties. The realization of the bound in (3.30) is nicely visible. On the other hand, the contour plots show also that the situation for the extraction of  $\gamma$  is not as fortunate as in the case of the  $B_d \rightarrow \pi^+ \pi^-$ ,  $B_s \rightarrow K^+ K^-$  system discussed in Section 2. Moreover, further constraints arise from  $\cos \delta_s$ , which has to agree with the positive sign of  $\cos \delta$ . A closer look at (3.42) shows, that this is only the case for the lower branches of the  $\gamma$ - $r_s$  contours, i.e. for the minus (plus) signs in (3.33) ((3.42)). Combining all this information, we arrive at the following ranges:

$$26^\circ \leq \gamma \leq 70^\circ, \quad 0.07 \leq r \leq 0.12. \quad (3.44)$$

Since only the lower branches of the  $\gamma$ - $r_s$  contours are effective because of the constraint on  $\delta_s$ , a solution for  $\gamma$  around  $65^\circ$  requires in particular an increase of  $R_s$ , which still suffers from significant uncertainties, and would welcome an increase of  $R$  as well, which is known at the 5% level. In principle, such an effect could be due to the  $\rho_{\pi K}$  parameter in (3.8). However, the analysis of Subsection 3.2 demonstrates that this corresponds to only a few percent. Interestingly, it shifts  $R$  in the right direction, but this effect is definitely much too small to cure the problem with  $R_s$ . If we consider the upper  $1\sigma$  values of  $R_s = 0.306$  and  $R = 0.948$ , we obtain the following values:

$$\gamma = 69.4^\circ, \quad r = 0.101, \quad \delta = 28.5^\circ, \quad \delta_s = 39.2^\circ, \quad (3.45)$$

which would look quite reasonable.

Using both  $U$ -spin relations in (3.3) simultaneously, the following expression can straightforwardly be derived from (3.28) and (3.38):

$$r = \sqrt{\epsilon \left[ \frac{R + R_s - 1 - \epsilon}{1 + \epsilon} \right]}. \quad (3.46)$$

In the case of the central values of the current experimental results, we obtain  $r = 0.06$ , whereas the upper  $1\sigma$  values yield  $r = 0.10$ . The advantage of the contours in the  $\gamma$ - $r_{(s)}$  plane is that the strong phases  $\delta$  and  $\delta_s$  can be extracted separately.

### 3.4 Interplay with the $B_s \rightarrow K^+ K^-$ , $B_d \rightarrow \pi^+ \pi^-$ Strategy

If we replace the strange spectator quark of  $B_s^0 \rightarrow K^+ K^-$  through a down quark, we obtain the  $B_d^0 \rightarrow \pi^- K^+$  decay, as can be seen in Fig. 1. Consequently, the only difference between the corresponding hadronic matrix elements is due to processes involving these spectator quarks: penguin annihilation and exchange topologies, which contribute to  $B_s^0 \rightarrow K^+ K^-$ , but are absent in the  $B_d^0 \rightarrow \pi^- K^+$  channel. These contributions, which are expected to play a minor rôle, can be probed through  $B_d \rightarrow K^+ K^-$  and  $B_s \rightarrow \pi^+ \pi^-$  decays [3]. The most recent data for the corresponding CP-averaged branching ratios read as follows [6]:

$$\text{BR}(B_d \rightarrow K^+ K^-) = (0.15_{-0.10}^{+0.11}) \times 10^{-6}, \quad (3.47)$$

$$\text{BR}(B_s \rightarrow \pi^+ \pi^-) = (0.53 \pm 0.51) \times 10^{-6}, \quad (3.48)$$

where the constraint on the  $B_s$  mode was recently obtained at the Tevatron [13]. Following Ref. [30], these measurements can be converted into constraints on strong amplitudes:

$$\begin{aligned} & \sqrt{\frac{1}{2} \left[ \frac{\text{BR}(B_d \rightarrow K^+ K^-)}{\text{BR}(B^\pm \rightarrow \pi^\pm \pi^0)} \right] \frac{\tau_{B^+}}{\tau_{B_d}}} \\ & \approx \left| \frac{\mathcal{E} - (\mathcal{PA})_{tu}}{\mathcal{T} + \mathcal{C}} \right| \sqrt{1 + 2\varrho_{\mathcal{PA}} \cos \vartheta_{\mathcal{PA}} \cos \gamma + \varrho_{\mathcal{PA}}^2} = 0.12_{-0.06}^{+0.04}, \end{aligned} \quad (3.49)$$

$$\sqrt{\frac{\epsilon}{2} \left[ \frac{\text{BR}(B_s \rightarrow \pi^+ \pi^-)}{\text{BR}(B^\pm \rightarrow \pi^\pm \pi^0)} \right] \frac{\tau_{B^+}}{\tau_{B_s}}} \approx \frac{1}{R_b} \left| \frac{(\mathcal{PA})_{tc}}{\mathcal{T} + \mathcal{C}} \right| = 0.05_{-0.04}^{+0.03}. \quad (3.50)$$

Here  $\mathcal{T} + \mathcal{C}$  describes the sum of colour-allowed and colour-suppressed tree topologies,  $\mathcal{E}$  is an exchange amplitude, whereas the  $(\mathcal{PA})_{tq}$  are the differences of penguin annihilation amplitudes with internal top and  $q \in \{u, c\}$  quarks. Finally,

$$\varrho_{\mathcal{PA}} e^{i\vartheta_{\mathcal{PA}}} \equiv \frac{1}{R_b} \left[ \frac{(\mathcal{PA})_{tc}}{\mathcal{E} - (\mathcal{PA})_{tu}} \right], \quad (3.51)$$

with  $R_b \approx 0.4$  denoting the side of the UT that is proportional to  $|V_{ub}/V_{cb}|$ . Consequently, the data from the  $B$  factories and the Tevatron do not indicate any anomalous behaviour of these topologies so that we will neglect them in the following discussion. Similar assumptions were made in the recent extractions of  $\gamma$  from  $B_d \rightarrow \pi^+ \pi^-$ ,  $B \rightarrow \pi K$  modes in Refs. [10, 49], yielding results that agree within the errors with our value of  $\gamma$  in (2.19).

Applying the  $SU(3)$  flavour symmetry, we may then identify the  $B_s^0 \rightarrow K^+ K^-$  and  $B_d^0 \rightarrow \pi^- K^+$  decay amplitudes [1, 21, 22], and obtain the simple relation:

$$r e^{i\delta} = \frac{\epsilon}{d} e^{i(\pi - \theta)}, \quad (3.52)$$

which allows us to convert (2.14) and (2.15) into their  $B_d^0 \rightarrow \pi^- K^+$  counterparts:

$$\gamma = (40.6_{-2.8}^{+3.0})^\circ, \quad r = 0.209_{-0.019}^{+0.027}, \quad \delta = (150.8_{-15.3}^{+13.3})^\circ, \quad (3.53)$$

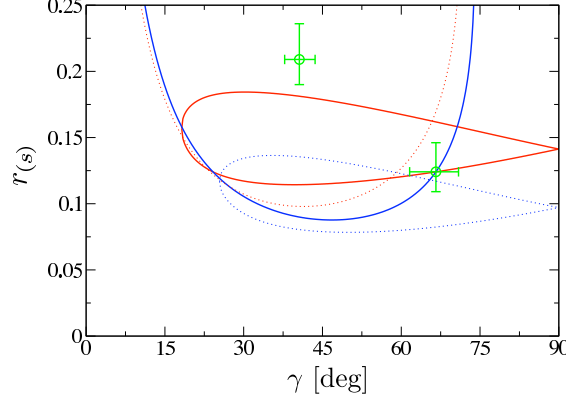


Figure 10: Future scenario for the contours in the  $\gamma$ - $r(s)$  plane, as discussed in the text. The dotted lines refer to the central values of the current data.

$$\gamma = (66.6^{+4.3}_{-5.0})^\circ, \quad r = 0.124^{+0.022}_{-0.015}, \quad \delta = (24.1^{+4.5}_{-11.1})^\circ. \quad (3.54)$$

In Fig. 9, we have included these values as the two points with error bars. We can nicely see that the  $\gamma$ - $r$  contour, which is fixed through  $R$  and  $A_0$ , clearly rules out (3.53), as we noted in Subsection 2.5. So we are left with the SM-like solution of (3.54), which would favour a slight increase of  $R$ , and quite a significant increase of  $R_s$ . In fact, if we calculate these quantities for that case, we obtain

$$R = 0.925^{+0.018}_{-0.021}, \quad R_s = 0.444^{+0.137}_{-0.084}, \quad (3.55)$$

where the errors are due to our input parameters. Converting the value of  $R_s$  into the  $B_s \rightarrow \pi^\pm K^\mp$  branching ratio yields

$$\text{BR}(B_s \rightarrow \pi^\pm K^\mp) = (9.4^{+3.3}_{-2.3}) \times 10^{-6}, \quad (3.56)$$

which is about  $1.6\sigma$  larger than the CDF result in (1.8). The prediction of the direct CP violation in  $B_d \rightarrow \pi^\mp K^\pm$  yields

$$\mathcal{A}_{\text{CP}}^{\text{dir}}(B_d \rightarrow \pi^\mp K^\pm) = +0.101^{+0.055}_{-0.047}, \quad (3.57)$$

with the same numerical value as the prediction of  $\mathcal{A}_{\text{CP}}^{\text{dir}}(B_s \rightarrow K^+ K^-)$  in Subsection 2.6. In fact, using the assumptions listed above, we expect

$$\mathcal{A}_{\text{CP}}^{\text{dir}}(B_s \rightarrow K^+ K^-) = \mathcal{A}_{\text{CP}}^{\text{dir}}(B_d \rightarrow \pi^\mp K^\pm) \stackrel{\text{exp}}{=} 0.095 \pm 0.013. \quad (3.58)$$

Moreover, we have  $\mathcal{A}_{\text{CP}}^{\text{dir}}(B_s \rightarrow \pi^\pm K^\mp) = -0.21$ , which is equal to our input parameter for the direct CP asymmetry of the  $B_d \rightarrow \pi^+ \pi^-$  channel. The agreement between (3.57) and the experimental value in (3.58) is remarkable, and disfavors large  $SU(3)$ -breaking corrections, in particular to the relations between strong phases (see Subsection 2.6). In Fig. 10, we show the corresponding situation in the  $\gamma$ - $r(s)$  plane as a future scenario for the evolution of the data.

Let us finally return to the CP-averaged branching ratios, where the relation

$$\frac{\text{BR}(B_s \rightarrow K^+ K^-)}{\text{BR}(B_d \rightarrow \pi^\mp K^\pm)} = \left[ \frac{M_{B_d}}{M_{B_s}} \frac{\Phi(M_K/M_{B_s}, M_K/M_{B_s})}{\Phi(M_\pi/M_{B_d}, M_K/M_{B_d})} \frac{\tau_{B_s}}{\tau_{B_d}} \right] \left( \frac{f_\pi}{f_K} \left| \frac{\mathcal{C}'}{\mathcal{C}} \right|_{\text{fact}} \right)^2 \quad (3.59)$$

allows us to extract

$$\left| \frac{\mathcal{C}'}{\mathcal{C}} \right|_{\text{fact}}^{\text{exp}} = 1.42 \pm 0.14 \quad (3.60)$$

from the data. Within the uncertainties, this number agrees remarkably well with (2.12), and gives us further confidence into the corresponding form factors and the smallness of non-factorizable  $SU(3)$ -breaking effects. In analogy to (3.59), we also have

$$\frac{\text{BR}(B_s \rightarrow \pi^\pm K^\pm)}{\text{BR}(B_d \rightarrow \pi^+ \pi^-)} = \left[ \frac{M_{B_d}}{M_{B_s}} \frac{\Phi(M_\pi/M_{B_s}, M_K/M_{B_s})}{\Phi(M_\pi/M_{B_d}, M_\pi/M_{B_d})} \frac{\tau_{B_s}}{\tau_{B_d}} \right] \left( \frac{f_K}{f_\pi} \left| \frac{P_s}{P} \right|_{\text{fact}} \right)^2. \quad (3.61)$$

Using the numerical value in (3.5) with  $f_K/f_\pi = 1.22$ , we obtain

$$\text{BR}(B_s \rightarrow \pi^\pm K^\pm) = (7.5 \pm 1.2) \times 10^{-6}. \quad (3.62)$$

This prediction is a bit smaller than (3.56), but fully consistent within the errors. On the other hand, it is about  $1.4\sigma$  larger than the experimental value in (1.8), thereby giving further support for the observations made above and in Subsection 3.3. Using the  $U$ -spin relation in (3.6), the enhancement of the central value of  $\text{BR}(B_s \rightarrow \pi^\pm K^\pm)$  by a factor of 1.5 would suppress the central value of (1.10) to

$$\mathcal{A}_{\text{CP}}^{\text{dir}}(B_s \rightarrow \pi^\pm K^\mp) \sim -0.26, \quad (3.63)$$

which would further support the BaBar measurement in (1.7), as

$$\mathcal{A}_{\text{CP}}^{\text{dir}}(B_s \rightarrow \pi^\pm K^\mp) \approx \mathcal{A}_{\text{CP}}^{\text{dir}}(B_d \rightarrow \pi^+ \pi^-). \quad (3.64)$$

Since the form-factor ratio

$$\frac{f_\pi}{f_K} \left| \frac{\mathcal{C}'}{\mathcal{C}} \right|_{\text{fact}} = \frac{F_{B_s K}(M_K^2; 0^+)}{F_{B_d \pi}(M_\pi^2; 0^+)} \left( \frac{M_{B_s}^2 - M_K^2}{M_{B_d}^2 - M_\pi^2} \right) \quad (3.65)$$

is essentially equal to

$$\frac{f_K}{f_\pi} \left| \frac{P_s}{P} \right|_{\text{fact}} = \frac{F_{B_s K}(M_\pi^2; 0^+)}{F_{B_d \pi}(M_K^2; 0^+)} \left( \frac{M_{B_s}^2 - M_K^2}{M_{B_d}^2 - M_\pi^2} \right), \quad (3.66)$$

we arrive at the following relation, which does not depend on the form-factor ratios:<sup>2</sup>

$$\text{BR}(B_s \rightarrow \pi^\pm K^\pm) = \left[ \frac{\text{BR}(B_s \rightarrow K^+ K^-)}{\text{BR}(B_d \rightarrow \pi^\mp K^\pm)} \right] \text{BR}(B_d \rightarrow \pi^+ \pi^-) = (6.5 \pm 1.3) \times 10^{-6}. \quad (3.67)$$

If we increase  $\text{BR}(B_s \rightarrow K^+ K^-)$  by a factor of 1.15 in order to get full agreement between the central values of (3.60) and (2.12) (which is below a  $1\sigma$  fluctuation and would have a small impact on the  $\gamma$  determination in Section 2), we would arrive again at (3.62). Instead of predicting this branching ratio, we may perform an experimental test of non-factorizable  $SU(3)$ -breaking effects:

$$\Delta_{SU(3)}^{\text{NF}} \equiv 1 - \left[ \frac{\text{BR}(B_s \rightarrow K^+ K^-)}{\text{BR}(B_s \rightarrow \pi^\pm K^\pm)} \right] \left[ \frac{\text{BR}(B_d \rightarrow \pi^+ \pi^-)}{\text{BR}(B_d \rightarrow \pi^\mp K^\pm)} \right] = -0.3 \pm 0.4. \quad (3.68)$$

In view of the large uncertainties, this relation is not yet very constraining. However, it should provide valuable insights as the data improve.

---

<sup>2</sup>In (3.59) and (3.61), actually  $F_{B_d \pi}(M_K^2; 0^+)$  and  $F_{B_d \pi}(M_\pi^2; 0^+)$  enter, respectively.



## 4 Conclusions

We have performed an analysis of the  $U$ -spin-related decays  $B_d \rightarrow \pi^+\pi^-$ ,  $B_s \rightarrow K^+K^-$  and  $B_d \rightarrow \pi^\mp K^\pm$ ,  $B_s \rightarrow \pi^\pm K^\mp$ , exploring the implications of the current  $B$ -factory data and the first results on the  $B_s$  modes from the Tevatron and setting the stage for the data taking at the LHC. The main results can be summarized as follows:

- The analysis of the  $B_d \rightarrow \pi^+\pi^-$ ,  $B_s \rightarrow K^+K^-$  system favours the BaBar measurement of the direct CP violation in the former decay. We have performed the first determination of  $\gamma$  by using only  $U$ -spin-related decays, and found a particularly fortunate situation, yielding  $\gamma = (66.6^{+4.3+4.0+0.1}_{-5.0-3.0-0.2})^\circ$ , where the first errors reflect the uncertainties of the input quantities, and the second and third errors show the sensitivity to generous non-factorizable  $U$ -spin-breaking corrections.
- This value of  $\gamma$  is in excellent agreement with the SM fits of the UT. We have shown how discrete ambiguities can be resolved through  $\mathcal{A}_{\text{CP}}^{\text{mix}}(B_s \rightarrow K^+K^-)$ , which has not yet been measured. However, may use alternatively the observables of the  $B_d \rightarrow \pi^\mp K^\pm$ ,  $B^\pm \rightarrow \pi^\pm K$  modes, leaving us with the result for  $\gamma$  given above.
- The next important step in this analysis will be the observation of mixing-induced CP violation in the  $B_s^0 \rightarrow K^+K^-$  decay. In the SM, we predict this asymmetry as  $\mathcal{A}_{\text{CP}}^{\text{mix}}(B_s \rightarrow K^+K^-) = -0.246^{+0.036+0.008+0.051}_{-0.030-0.007-0.023}$ , where the second and third errors illustrate again the impact of large non-factorizable  $U$ -spin-breaking corrections. We have also explored the impact of CP-violating NP contributions to  $B_s^0$ - $\bar{B}_s^0$  mixing on this observable, which affect it sensitively. Moreover, we pointed out that the measurements of  $\mathcal{A}_{\text{CP}}^{\text{mix}}(B_s \rightarrow K^+K^-)$  and  $\sin \phi_s$  through  $B_s \rightarrow J/\psi\phi$  will allow an *unambiguous* determination of the  $B_s^0$ - $\bar{B}_s^0$  mixing phase  $\phi_s$ .
- Using the results of our analysis, the measurement of the  $B_s \rightarrow K^+K^-$  lifetime through an untagged data sample can be converted into the width difference  $\Delta\Gamma_s$ . In the SM, the corresponding key observable is given by  $\mathcal{A}_{\Delta\Gamma}(B_s \rightarrow K^+K^-) = -0.964^{+0.011}_{-0.007}$ , which is essentially unaffected by  $U$ -spin-breaking corrections.
- In the case of the  $B_d \rightarrow \pi^\mp K^\pm$ ,  $B_s \rightarrow \pi^\pm K^\mp$  system, the determination of  $\gamma$  requires an additional input, which is provided by  $B^\pm \rightarrow \pi^\pm K$ . In contrast to the  $B_d \rightarrow \pi^+\pi^-$ ,  $B_s \rightarrow K^+K^-$  system, we have then also to make additional dynamical assumptions. In particular, another hadronic parameter enters  $B^\pm \rightarrow \pi^\pm K$ , which is doubly Cabibbo-suppressed, but could be enhanced by final-state interaction effects. Using the  $B$ -factory data for  $B^\pm \rightarrow K^\pm K$  modes, we have shown that this is actually not the case, and that these effects can safely be neglected. This does also support the neglect of colour-suppressed EW penguins.
- Using  $\text{BR}(B^\pm \rightarrow \pi^\pm K)$  to normalize the branching ratios of  $B_d \rightarrow \pi^\mp K^\pm$  and  $B_s \rightarrow \pi^\pm K^\mp$ , we have introduced two quantities  $R$  and  $R_s$ , respectively. In the case of  $R$ , the bound of  $\gamma \leq (71.5^{+5.3}_{-4.3})^\circ$  is implied, which puts a constraint on this UT angle in a phenomenologically interesting region. If we combine  $R$  and  $R_s$  with the direct CP asymmetries of the  $B_d \rightarrow \pi^\mp K^\pm$  and  $B_s \rightarrow \pi^\pm K^\mp$  modes,

respectively, we can extract  $\gamma$ , a hadronic parameter  $r$ , and two strong phases with the help of the  $U$ -spin symmetry. The situation resulting from the current data leaves us with  $26^\circ \leq \gamma \leq 70^\circ$ , and is not as favourable as in the case of  $B_d \rightarrow \pi^+\pi^-$ ,  $B_s \rightarrow K^+K^-$ . Moreover, this analysis favours an increase of the  $R_s$  ratio.

- If we neglect exchange and penguin annihilation topologies – the most recent bounds from the  $B_d \rightarrow K^+K^-$  and  $B_s \rightarrow \pi^+\pi^-$  data do not indicate any anomalous enhancement – we obtain an interesting interplay between the  $B_d \rightarrow \pi^+\pi^-$ ,  $B_s \rightarrow K^+K^-$  and  $B_d \rightarrow \pi^\mp K^\pm$ ,  $B_s \rightarrow \pi^\pm K^\mp$  systems. This allows us to resolve the ambiguity in the extraction of  $\gamma$  from the former decays, as noted above, and to determine an  $SU(3)$ -breaking form-factor ratio from the data, which agrees with the result of a recent QCD sum-rule calculation used in our analysis, and disfavors large non-factorizable effects. Moreover, we can also make predictions for  $\text{BR}(B_s \rightarrow \pi^\pm K^\mp)$ , which point towards an increase with respect to the current CDF central value.

The  $U$ -spin extraction of  $\gamma$  from the  $B_d \rightarrow \pi^+\pi^-$ ,  $B_s \rightarrow K^+K^-$  system is already for the first Tevatron data one of the most accurate determinations on the market, and can be subsequently further optimized. In our analysis, we obtain a remarkable agreement with the SM picture of CP violation. Thanks to the start of the LHC, we will soon enter a new era for the exploration of the  $B_s$ -meson system. The LHCb experiment will then allow us to obtain a much sharper picture of the strategy discussed in this paper and to exploit its full physics potential. Moreover, also precision measurements of  $\gamma$  from tree-level processes will become possible, which are another – still missing – key element for the search of NP. It will be very interesting to compare all these measurements with one another and to confront the Kobayashi–Maskawa mechanism of CP violation with another round of stringent tests.

## References

- [1] R. Fleischer, *Phys. Lett.* **B459** (1999) 306.
- [2] N. Cabibbo, *Phys. Rev. Lett.* **10** (1963) 531; M. Kobayashi and T. Maskawa, *Prog. Theor. Phys.* **49** (1973) 652.
- [3] M. Gronau, J.L. Rosner and D. London, *Phys. Rev. Lett.* **73** (1994) 21; M. Gronau, O.F. Hernandez, D. London and J.L. Rosner, *Phys. Rev.* **D50** (1994) 4529.
- [4] R. Fleischer, lectures given at European School of High-Energy Physics, Kitzbühel, Austria, 21 August – 3 September 2005 [hep-ph/0608010].
- [5] M. Gronau and J.L. Rosner, *Phys. Lett.* **B482** (2000) 7.
- [6] E. Barberio *et al.* [Heavy Flavor Averaging Group (HFAG)], hep-ex/0603003; for the most recent updates, see <http://www.slac.stanford.edu/xorg/hfag/>.
- [7] B. Aubert *et al.* [BaBar Collaboration], *Phys. Rev. Lett.* **93** (2004) 131801; Y. Chao *et al.* [Belle Collaboration], *Phys. Rev. Lett.* **93** (2004) 191802.

- [8] B. Aubert *et al.* [BaBar Collaboration], BABAR-PUB-07-013 [hep-ex/0703016].
- [9] K. Abe [Belle Collaboration], BELLE-CONF-0649 [hep-ex/0608035].
- [10] R. Fleischer, S. Recksiegel and F. Schwab, *Eur. Phys. J. C* (2007) DOI 10.1140/epjc/s10052-007-0277-8 [hep-ph/0702275].
- [11] K. Abe *et al.* [Belle Collaboration], hep-ex/0610003.
- [12] A. Abulencia *et al.* [CDF Collaboration], *Phys. Rev. Lett.* **97** (2006) 211802.
- [13] G. Punzi, talk at CKM2006, 12–16 December 2006, Nagoya, Japan [hep-ex/0703029].
- [14] T. Nakada, talk at CKM 2006, Nagoya, Japan, 12–16 December 2006; A. Schopper, Proceedings of FPCP 2006, Vancouver, British Columbia, Canada, 9–12 April 2006, pp 042 [hep-ex/0605113].
- [15] M. Beneke and M. Neubert, *Nucl. Phys.* **B675** (2003) 333.
- [16] A.R. Williamson and J. Zupan, *Phys. Rev.* **D74** (2006) 014003 [Erratum-ibid. **D74** (2006) 03901].
- [17] A. Ali, G. Kramer, Y. Li, C.-D. Lü, Y.L. Shen, W. Wang and Y.M. Wang, DESY-07-021 [hep-ph/0703162].
- [18] L. Wolfenstein, *Phys. Rev. Lett.* **51** (1983) 1945.
- [19] M. Bauer, B. Stech and M. Wirbel, *Z. Phys.* **C29** (1985) 637 and **C34** (1987) 103.
- [20] A. Khodjamirian, T. Mannel and M. Melcher, *Phys. Rev.* **D70** (2004) 094002.
- [21] R. Fleischer, *Eur. Phys. J.* **C16** (2000) 87.
- [22] R. Fleischer and J. Matias, *Phys. Rev.* **D66** (2002) 054009.
- [23] G. Balbi *et al.*, CERN-LHCb/2003-123 and 124; R. Antunes Nobrega *et al.* [LHCb Collaboration], *Reoptimized LHCb Detector, Design and Performance*, Technical Design Report 9, CERN/LHCC 2003-030; J. Nardulli, talk at CKM 2006, Nagoya, Japan, 12–16 December 2006.
- [24] M. Bona *et al.* [UTfit Collaboration], *JHEP* **0507** (2005) 028; for the most recent updates, see <http://utfit.roma1.infn.it/>.
- [25] J. Charles *et al.* [CKMfitter Group], *Eur. Phys. J.* **C41** (2005) 1; for the most recent updates, see <http://ckmfitter.in2p3.fr/>.
- [26] R. Fleischer and I. Dunietz, *Phys. Rev.* **D55** (1997) 259.
- [27] I. Dunietz, R. Fleischer and U. Nierste, *Phys. Rev.* **D63** (2001) 114015.
- [28] CDF collaboration, CDF Note 06-01-26 (2006).

- [29] R. Fleischer, *Nucl. Phys.* **B671** (2003) 459.
- [30] A.J. Buras, R. Fleischer, S. Recksiegel and F. Schwab, *Phys. Rev. Lett.* **92** (2004) 101804; *Nucl. Phys.* **B697** (2004) 133.
- [31] V.M. Abazov *et al.* [D0 Collaboration], *Phys. Rev. Lett.* **97** (2006) 021802.
- [32] A. Abulencia *et al.* [CDF Collaboration], *Phys. Rev. Lett.* **97** (2006) 242003.
- [33] P. Ball and R. Fleischer, *Eur. Phys. J.* **C48** (2006) 413.
- [34] M. Ciuchini and L. Silvestrini, *Phys. Rev. Lett.* **97** (2006) 021803; Z. Ligeti, M. Papucci and G. Perez, *Phys. Rev. Lett.* **97** (2006) 101801; Y. Grossman, Y. Nir and G. Raz, *Phys. Rev. Lett.* **97** (2006) 151801.
- [35] A.S. Dighe, I. Dunietz and R. Fleischer, *Eur. Phys. J.* **C6** (1999) 647.
- [36] R. Fleischer and J. Matias, *Phys. Rev.* **D61** (2000) 074004.
- [37] V.M. Abazov *et al.* [D0 Collaboration], *Phys. Rev. Lett.* **98** (2007) 121801.
- [38] Y. Grossman, *Phys. Lett.* **B380** (1996) 99.
- [39] A. Lenz and U. Nierste, hep-ph/0612167.
- [40] A.J. Buras, R. Fleischer and T. Mannel, *Nucl. Phys.* **B533** (1998) 3; A.F. Falk, A.L. Kagan, Y. Nir and A.A. Petrov, *Phys. Rev.* **D57** (1998) 4290; M. Neubert, *JHEP* **9902** (1999) 014.
- [41] R. Fleischer, *Eur. Phys. J.* **C6** (1999) 451.
- [42] B. Aubert *et al.* [BaBar Collaboration], *Phys. Rev. Lett.* **97** (2006) 171805.
- [43] K. Abe *et al.* [Belle Collaboration], BELLE-CONF-0633 [hep-ex/0608049].
- [44] R. Fleischer and S. Recksiegel, *Phys. Rev.* **D71** (2005) 051501 (R).
- [45] P. Ball and R. Zwicky, *Phys. Rev.* **D71** (2005) 014015.
- [46] R. Fleischer and T. Mannel, *Phys. Rev.* **D57** (1998) 2752.
- [47] W.M. Yao *et al.* [Particle Data Group], *J. Phys.* **G33** (2006) 1.
- [48] M. Gronau and J.L. Rosner, *Phys. Rev.* **D57** (1998) 6843.
- [49] M. Gronau and J.L. Rosner, arXiv:0704.3459 [hep-ph].